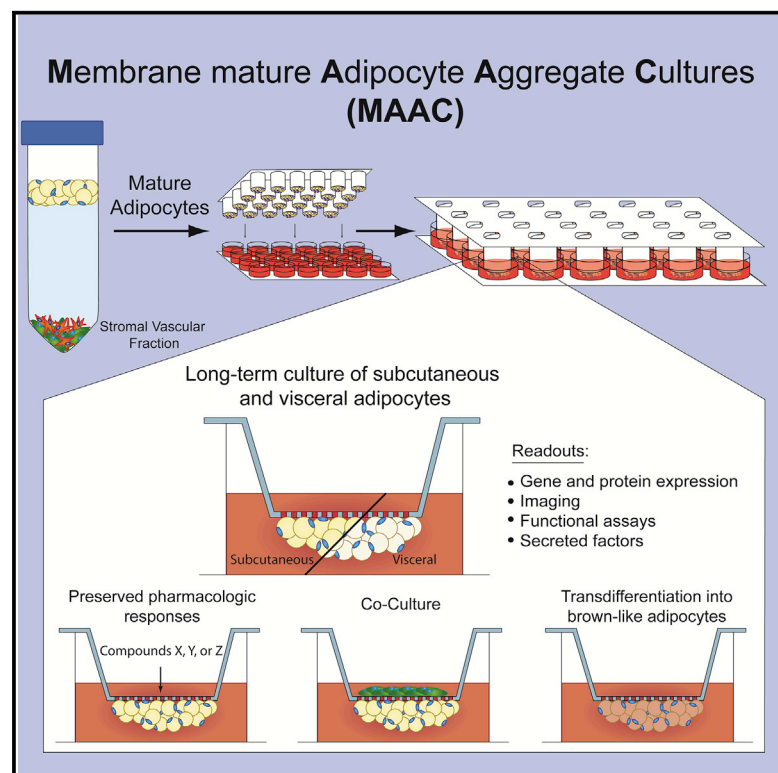


## Mature Human White Adipocytes Cultured under Membranes Maintain Identity, Function, and Can Transdifferentiate into Brown-like Adipocytes

### Graphical Abstract



### Authors

Matthew J. Harms, Qian Li, Sunjae Lee, ..., Adil Mardinoglu, Kirsty L. Spalding, Jeremie Boucher

### Correspondence

jeremie.boucher@astrazeneca.com

### In Brief

Mature adipocytes are notoriously difficult to culture. Here, Harms et al. describe a robust method for the long-term culture of mature white adipocytes under permeable membranes, which preserves adipocyte identity and function. Using this approach, they also show that human mature white adipocytes can transdifferentiate into brown-like adipocytes.

### Highlights

- Mature adipocytes cultured as MAAC preserve cellular identity and function
- Subcutaneous and visceral adipocytes can be cultured as MAAC
- Adipocytes from lean and obese donors can be cultured
- Human mature white adipocytes can transdifferentiate into brown-like adipocytes



# Mature Human White Adipocytes Cultured under Membranes Maintain Identity, Function, and Can Transdifferentiate into Brown-like Adipocytes

Matthew J. Harms,<sup>1</sup> Qian Li,<sup>2</sup> Sunjae Lee,<sup>3,9</sup> Cheng Zhang,<sup>3</sup> Bengt Kull,<sup>1</sup> Stefan Hallen,<sup>1</sup> Anders Thorell,<sup>4</sup> Ida Alexandersson,<sup>1</sup> Carolina E. Hagberg,<sup>5</sup> Xiao-Rong Peng,<sup>1</sup> Adil Mardinoglu,<sup>3,6</sup> Kirsty L. Spalding,<sup>2,5</sup> and Jeremie Boucher<sup>1,7,8,10,\*</sup>

<sup>1</sup>Cardiovascular, Renal and Metabolism, IMED Biotech Unit, AstraZeneca, Gothenburg, Sweden

<sup>2</sup>Department of Cell and Molecular Biology (CMB), Karolinska Institutet, Stockholm 17177, Sweden

<sup>3</sup>Science for Life Laboratory, KTH-Royal Institute of Technology, Stockholm 17121, Sweden

<sup>4</sup>Department of Clinical Sciences, Danderyds Hospital, Karolinska Institutet and Department of Surgery, Ersta Hospital, Stockholm 11691, Sweden

<sup>5</sup>Karolinska Institutet/AstraZeneca Integrated Cardio Metabolic Centre (KI/AZ ICMC), Department of Medicine, Karolinska Institutet, Stockholm 17176, Sweden

<sup>6</sup>Centre for Host-Microbiome Interactions, Faculty of Dentistry, Oral & Craniofacial Sciences, King's College London, London SE1 9RT, United Kingdom

<sup>7</sup>The Lundberg Laboratory for Diabetes Research, University of Gothenburg, Sweden

<sup>8</sup>Wallenberg Centre for Molecular and Translational Medicine, University of Gothenburg, Sweden

<sup>9</sup>Present address: Centre for Host-Microbiome Interactions, Faculty of Dentistry, Oral & Craniofacial Sciences, King's College London, London SE1 9RT, United Kingdom

<sup>10</sup>Lead Contact

\*Correspondence: [jeremie.boucher@astrazeneca.com](mailto:jeremie.boucher@astrazeneca.com)

<https://doi.org/10.1016/j.celrep.2019.03.026>

## SUMMARY

White adipose tissue (WAT) is a central factor in the development of type 2 diabetes, but there is a paucity of translational models to study mature adipocytes. We describe a method for the culture of mature white adipocytes under a permeable membrane. Compared to existing culture methods, MAAC (membrane mature adipocyte aggregate cultures) better maintain adipogenic gene expression, do not dedifferentiate, display reduced hypoxia, and remain functional after long-term culture. Subcutaneous and visceral adipocytes cultured as MAAC retain depot-specific gene expression, and adipocytes from both lean and obese patients can be cultured. Importantly, we show that rosiglitazone treatment or PGC1 $\alpha$  overexpression in mature white adipocytes induces a brown fat transcriptional program, providing direct evidence that human adipocytes can transdifferentiate into brown-like adipocytes. Together, these data show that MAAC are a versatile tool for studying phenotypic changes of mature adipocytes and provide an improved translational model for drug development.

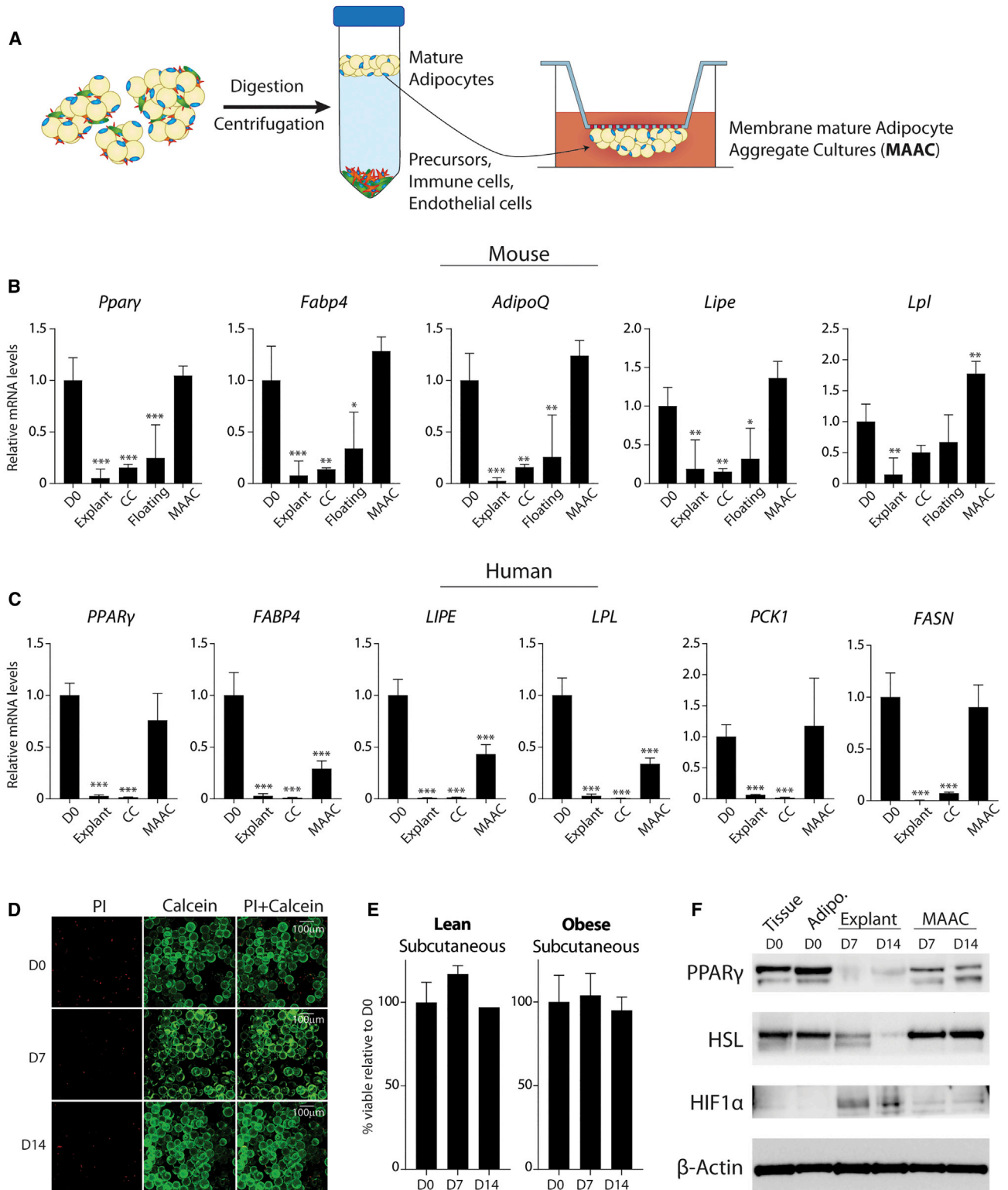
## INTRODUCTION

Adipose tissue plays a central role in the development of insulin resistance and type 2 diabetes (T2D). Under caloric excess, adipocytes undergo hypertrophy to clear lipids from circulation;

however, this finite lipid-buffering capacity can become exhausted, leading to lipid accumulation in non-adipose tissues (Guilherme et al., 2008; Lotta et al., 2017; Rosen and Spiegelman, 2014; Samuel and Shulman, 2012). This limited storage capacity of adipocytes and subsequent overflow of lipids into other tissues has been identified as a key etiological and genetic component in the development of diabetes and insulin-resistant cardiometabolic disease (Lotta et al., 2017). Thiazolidinediones (TZDs) are a class of antidiabetic drugs that act on adipocytes through PPAR $\gamma$ , the master regulator of adipogenesis, showing that modulating adipose tissue function is a viable strategy to treat T2D (Tontonoz and Spiegelman, 2008). Unfortunately, concerns about side effects have reduced the use of TZDs in the clinic (Ahmadian et al., 2013; Yki-Järvinen, 2004), necessitating the development of new drugs without side effects. Another attractive therapeutic avenue for treating T2D is transforming energy-storing white adipocytes into thermogenic brown-like adipocytes or activating uncoupling protein 1 (UCP1) in existing brown adipose tissue (BAT) (Harms and Seale, 2013).

The lack of translational *in vitro* adipocyte models is one of the main obstacles for the development of new transformational medicines that act on adipose for the treatment of T2D and obesity. The *ex vivo* culture of pieces of whole adipose tissue, also called explants, is associated with a rapid phenotype loss driven by hypoxia and inflammation (Fain et al., 2010; Gesta et al., 2003), and studies using this model often do not take into account the inherent changes that occur in explants over time compared to the starting material. Another method utilizes the natural buoyant properties of freshly isolated mature adipocytes, which float to the top of culture medium and do not attach at the bottom of wells or flasks. By completely filling a flask with culture medium, the floating adipocytes contact the top of the





(legend on next page)

chamber and become adherent ceiling cultures (CCs) after a couple of days (Sugihara et al., 1987; Sugihara et al., 1986). However, adipocytes cultured this way rapidly dedifferentiate into fibroblast-like cells (Adebonojo, 1975; Asada et al., 2011; Lesnard et al., 2015; Shen et al., 2011; Sugihara et al., 1989; Wei et al., 2013).

As a result of the aforementioned technical challenges, research on adipocytes is conducted almost exclusively using adipocytes differentiated *in vitro* from precursors. Primary preadipocytes and, more commonly, the mouse cell lines 3T3-L1, 3T3-F442A, and C3H10T1/2, which have been immortalized from non-adipose precursors but nevertheless possess adipogenic potential, are frequently used (Ruiz-Ojeda et al., 2016). Although these models have effectively expanded knowledge related to adipocyte development and function (Cristancho and Lazar, 2011; Rosen and MacDougald, 2006; Sarjeant and Stephens, 2012), they also have a number of limitations and gaps in translational relevance. Adipocytes differentiated *in vitro* are drastically smaller in size and never obtain the typical unilocular appearance that adipocytes *in vivo* possess. Additionally, *in vitro* adipocyte differentiation is a complex process involving the transient expression of many transcription factors (Siersbæk et al., 2012) that requires the addition of an extensive and unphysiological hormonal cocktail (Wang et al., 2014). Furthermore, *in vitro* adipocyte differentiation can be highly inconsistent as many factors can impact the ability of a preadipocyte to differentiate, including confluence, cell passage number, serum source and lot number, presence of mycoplasma, and reagent stability (Gregoire et al., 1998; McBeath et al., 2004; Ruiz-Ojeda et al., 2016; Wang et al., 2014).

Here, we developed a method for the long-term culture of mature adipocytes that mitigates the shortcomings of current methods and has improved translational relevance by culturing freshly isolated mature adipocytes underneath permeable small-pored membrane inserts (Figure S1A). We rationalized that the porous mesh would facilitate improved access to nutrients and oxygen, the more pliable membrane would better mimic the *in vivo* environment, and the small surface area would prevent the adipocytes from spreading and allow a 3D formation. We found that membrane mature adipocyte aggregate cultures (MAAC) are superior to other culture methods at preserving mature adipocyte identity and function. MAAC maintain a transcriptional profile that is closer to the starting material than all other methods tested, respond to both insulin and lipolytic stimuli, and are able to crosstalk with co-cultured macrophages. Importantly, using this adipocyte culture method, we provide

direct evidence that mature human subcutaneous white adipocytes have the capability to transdifferentiate into thermogenic brown-like adipocytes.

## RESULTS

### MAAC Preserve an Adipocyte Gene Signature

Mature adipocytes isolated from the subcutaneous adipose tissue of 6-week-old CD1 mice were directly pipetted onto the underside of a membrane and lowered into a well containing medium (Figure 1A; Figure S6). The buoyancy of the mature adipocytes maintains alignment and stable contact with the membrane, as well as facilitating the formation of 3D adipocyte aggregates. Adipose tissue explants, CC of mature adipocytes, and floating adipocytes without the use of a membrane, were used as culture comparisons. After culture for 7 days, transcript levels of adipocyte markers *Ppar $\gamma$* , *Fabp4*, and *AdipoQ* were decreased by over 95%, 85%, and 75% in explants, CC, and floating adipocytes, respectively, indicating that explants and mature adipocytes cultured according to standard methods undergo a rapid phenotype loss (Figure 1B). By contrast, adipocytes cultured under membranes maintained high expression of *Ppar $\gamma$* , *Fabp4*, and *AdipoQ*, similar to freshly isolated day 0 (D0) control cells. A time course revealed that the explant model undergoes a rapid >20-fold loss of *Ppar $\gamma$* , *Fabp4*, *AdipoQ*, *Lipe*, and *Lpl* within 3 days, whereas floating cells maintain approximately 50% of their adipogenic signature for 3 days but experience a 3- to 10-fold loss of expression of adipocyte markers by day 7 (Figure S1B). By contrast, MAAC had a 2-fold or less reduction in adipocyte gene expression by either day 3 or 7 compared to levels from the starting material.

Human subcutaneous adipocytes also maintained their phenotype when cultured under membranes. Human MAAC displayed a less than 3-fold decrease in expression of key adipogenic genes, such as *PPAR $\gamma$* , *FABP4*, and *LIPe*, among others, even after 2 weeks in culture, whereas explants and adipocyte CC displayed >20-fold decreases (Figure 1C). The morphology of MAAC after 2 weeks in culture was also indistinguishable from the starting adipocyte material (D0), whereas the adipocytes from the CCs underwent rapid dedifferentiation, which is in agreement with the literature (Asada et al., 2011; Sugihara et al., 1986; Wei et al., 2013) (Figure 1D; Figure S1C). Remarkably, MAAC showed little cell death even after 2 weeks of culture, as visualized by calcein-acetoxymethyl (AM) and propidium iodide (PI) staining, displaying numbers similar to the PI-positive cells measured in freshly isolated adipocytes (Figure 1D). This

### Figure 1. Membrane Culture of Adipocytes Maintains Viability and Preserves Mature Adipocyte Gene Expression

(A) Model depicting the use of membranes to culture mature adipocytes.

(B) mRNA levels of adipogenic genes from mouse subcutaneous adipocytes cultured in different methods for 7 days. D0, freshly isolated adipocytes snap frozen without culture; explants; CC, adipocyte ceiling cultures in T25 flasks; floating, floating adipocytes; MAAC, membrane mature adipocytes aggregate cultures (mean  $\pm$  SD; n = 4; CC, n = 3).

(C) mRNA levels of adipogenic genes from human subcutaneous D0 cells, adipose tissue explants, CC, and MAAC cultured for 2 weeks (mean  $\pm$  SD; D0, n = 6; explant, n = 5; CC, n = 4; MAAC, n = 6).

(D) Viability (calcein-AM and propidium iodide) staining of human adipocytes before culture (D0) and after culture for 7 and 14 days under membranes.

(E) Average percentage of viable cells after 7 and 14 days relative to freshly isolated subcutaneous adipocytes from lean and obese patients measured by staining with Hoechst 33342/PI (mean  $\pm$  SD; lean, n = 2; obese, n = 3).

(F) Western blot analysis of PPAR $\gamma$ , HSL, HIF1 $\alpha$ , and  $\beta$ -Actin in fresh human adipose tissue, isolated adipocytes (D0), explants, and MAAC cultured for 1 and 2 weeks. \*p < 0.05; \*\*p < 0.01; \*\*\*p < 0.001.

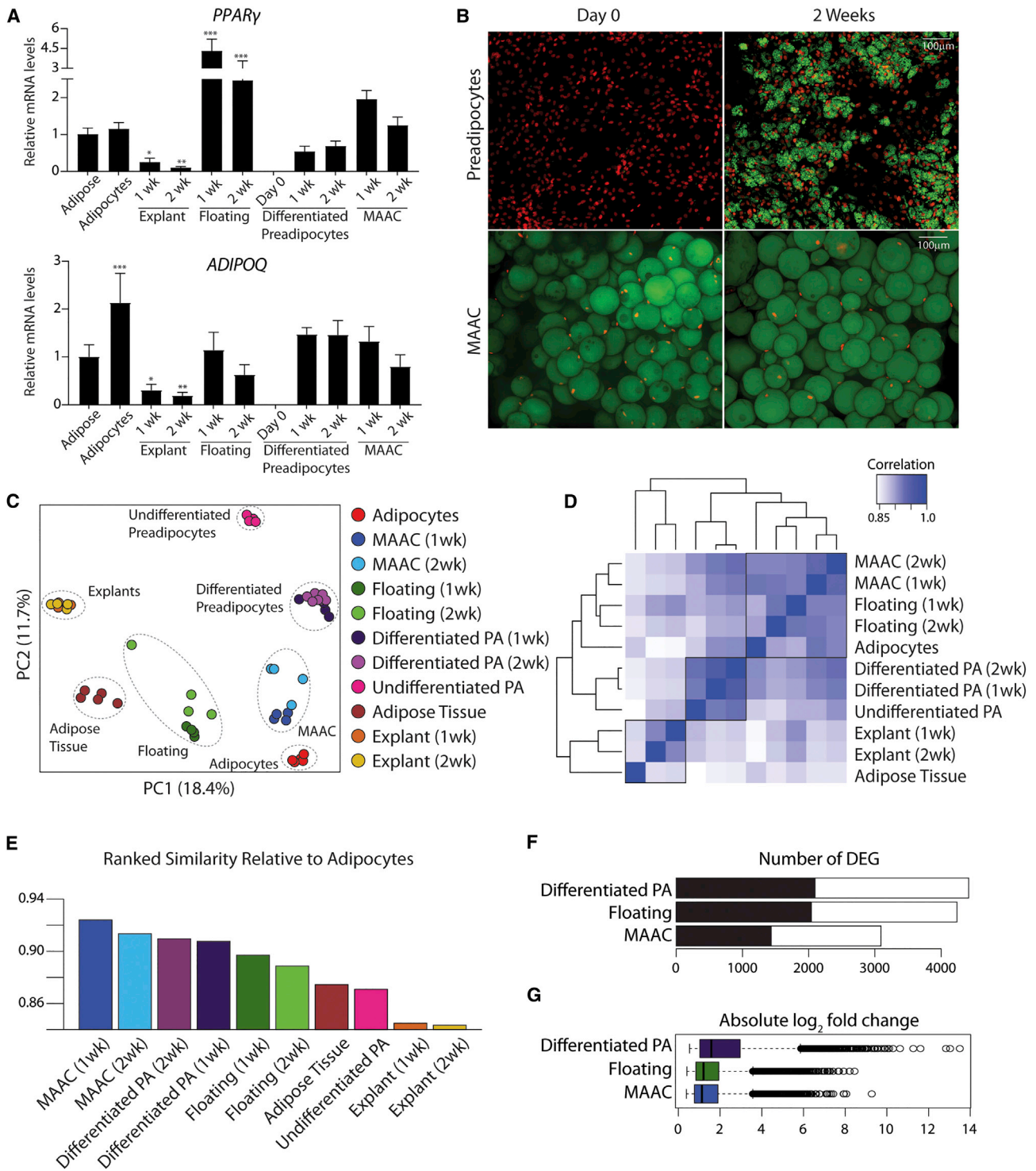


**Figure 2. Unbiased RNA-Seq Indicates That the Gene Expression Profile of MAAC Is the Most Similar to Uncultured Adipocytes**

(A) mRNA levels of adipogenic genes of adipose tissue snap frozen at the hospital, Day 0 isolated adipocytes (D0), explants, floating adipocytes, differentiated preadipocytes (PA), and MAAC cultured for 1 or 2 weeks (mean  $\pm$  SD; adipose tissue, n = 5; D0 adipocytes, n = 5; explant 1 week, n = 4; explant 2 weeks, n = 4; floating 1 week, n = 4; floating 2 weeks, n = 4; undifferentiated preadipocytes, n = 6; differentiated preadipocytes 1 week, n = 4; differentiated preadipocytes 2 weeks, n = 8; MAAC 1 week, n = 4; MAAC 2 weeks, n = 4). \*p < 0.05, \*\*p < 0.01, \*\*\*p < 0.001.

(B) Imaging comparing preadipocytes and MAAC at D0 and after 14 days in culture. Green, Bodipy (lipid); red, Hoechst 33342 (nuclei).

(legend continued on next page)

was true in adipocytes from both lean and obese patients: 96% of adipocytes from lean patients and 94% from obese patients remained viable after 2 weeks of culture (Figure 1E; Figure S1D). PPAR $\gamma$  and HSL protein expression were maintained consistently over the 2-week culture period under membranes, whereas explants displayed a robust and time-dependent decrease, similar to what was observed at the mRNA level (Figure 1F). Moreover, the adipose tissue explants showed a time-dependent increase in the protein levels of hypoxia-induced factor 1 $\alpha$  (HIF-1 $\alpha$ ), indicating hypoxic stress. By contrast, MAAC maintained low HIF-1 $\alpha$  levels. We hypothesized that the porous membrane allows adipocytes to maintain their adipogenic expression program by obviating hypoxic stress. To test this, MAAC and explants were cultured at normoxic and hypoxic conditions for 3 days and 1 week. The culture of MAAC for 3 days in hypoxic conditions triggered a >70% decrease of key adipogenic genes, including PPAR $\gamma$  and FABP4, which decreased even further after an additional 4 days of culture, reaching the low levels observed in adipose tissue explants cultured at normoxia (Figure S1E). Together, these results indicate that culture of mouse or human subcutaneous adipocytes under a permeable membrane is superior at maintaining a normal adipocyte gene signature relative to traditional mature adipocyte culture methods, such as CC and adipose tissue explants, at least in part by reduced hypoxic stress.

### Unbiased RNA Sequencing Indicates That MAAC Are the Most Similar to Uncultured Adipocytes

In order to compare the global gene expression changes in adipocytes cultured under different methods in an unbiased manner, we generated RNA sequencing (RNA-seq) data from the different models and included the benchmark of the field, adipocytes differentiated *in vitro* from precursors. Preadipocytes, mature adipocytes, and adipose tissue explants were all obtained from the same patient and cultured for 1 and 2 weeks. As described in Figure 1, the explant model displayed a rapid and robust decrease in the expression of adipogenic genes, such as PPAR $\gamma$ , ADIPOQ, LPL, and LIPE, whereas MAAC preserved expression, as measured by qPCR (Figures 2A and S2A). Interestingly, the preadipocytes differentiated *in vitro* for 2 weeks did not exhibit a significant difference in the expression of those genes compared to the starting adipocyte material, despite the striking difference in cell size and their multilocular lipid droplets (Figure 2B).

However, unbiased RNA-seq analysis revealed that MAAC are unequivocally the most similar to the starting material. Principal-component analysis (PCA) showed that through 2 weeks of culture, MAAC cluster most tightly with adipocytes freshly isolated on D0 (Figure 2C). Interestingly, floating cells also cluster closely with the control cells; however, the increase in culture time ap-

pears to cause more pronounced gene expression changes. Through the process of differentiation, preadipocytes become more mature adipocyte-like, but as evidenced by the distance along the second principal component (PC2), they still remain quite distinct. The adipose explants cluster most similarly to whole adipose tissue, as expected; however, the long separating distance along PC2 indicates that many changes occurred in the explant within 1 week. Hierarchical clustering based on average gene expression revealed that the MAAC and floating cells cluster with the D0 adipocyte controls, confirming the PCA (Figure 2D). Likewise, total ranked similarity to D0 adipocytes finds the MAAC at 1 and 2 weeks to be the most similar to isolated adipocytes, thereafter followed by the differentiated precursors, then floating adipocytes, whereas explants are more similar to adipose tissue (Figures 2E and S2B).

An analysis of 166 adipose-enriched genes (Table S1) selected from a published tissue-based map of the human proteome (Uhlén et al., 2015) facilitated directly comparing adipocytes and adipose tissue that is heterogeneous and contains more than just adipocytes. D0 adipocytes, MAAC, and adipose tissue had the highest levels of adipogenic gene expression, whereas the explants and undifferentiated precursors had the lowest levels (Figure S2C). The comparison of homogeneous adipocyte models revealed that relative to floating adipocytes and differentiated preadipocytes, MAAC had the fewest number of differentially expressed genes (DEG), and the DEGs had the lowest fold change (Figures 2F and 2G). Together, these data indicate that MAAC are the best model at preserving the gene expression profile of uncultured adipocytes.

### Membrane-Cultured Adipocytes Maintain Their Depot-Specific Expression Patterns

Adipocytes from different adipose tissue depots possess distinct gene expression signatures, with striking differences in the expression of developmental genes, such as SHOX2, EN1, NR2F1, and WT1 (Gesta et al., 2006; Waldén et al., 2012; Yamamoto et al., 2010; Zuriaga et al., 2017). To assess whether these differences are preserved after long term MAAC, human subcutaneous and visceral adipocytes were isolated from the same donor and cultured for 2 weeks under membranes. Similar to subcutaneous adipocytes, visceral adipocytes cultured under membranes also maintained the expression of the key adipocyte genes PPAR $\gamma$ , FABP4, ADIPOQ, and LPL (Figure 3A). Although the subcutaneous depot-enriched genes SHOX2 and EN1 were robustly detected in subcutaneous adipocytes, SHOX2 was not detected and EN1 displayed a 4-fold lower expression level in visceral adipocytes. This depot-specific differential expression was maintained through 2 weeks of culture (Figure 3B). Conversely, the visceral-enriched marker WT1 was not detected in subcutaneous samples, but was expressed in the visceral

(C) Principal component analysis of gene expression profiles from different adipocyte culture methods. Dashed gray lines demarcate the different experimental groups.

(D) Hierarchical clustering based on average gene expression compared by Pearson's correlation coefficients.

(E) Ranked similarity relative to D0 control adipocytes based on Pearson's correlation coefficients.

(F) Number of identified differentially expressed genes (DEGs) in differentiated preadipocytes, floating adipocytes, and MAAC [false discovery rate [FDR],  $<1 \times 10^{-3}$ ].

(G) Fold change in DEG in differentiated preadipocytes, floating adipocytes, and MAAC.

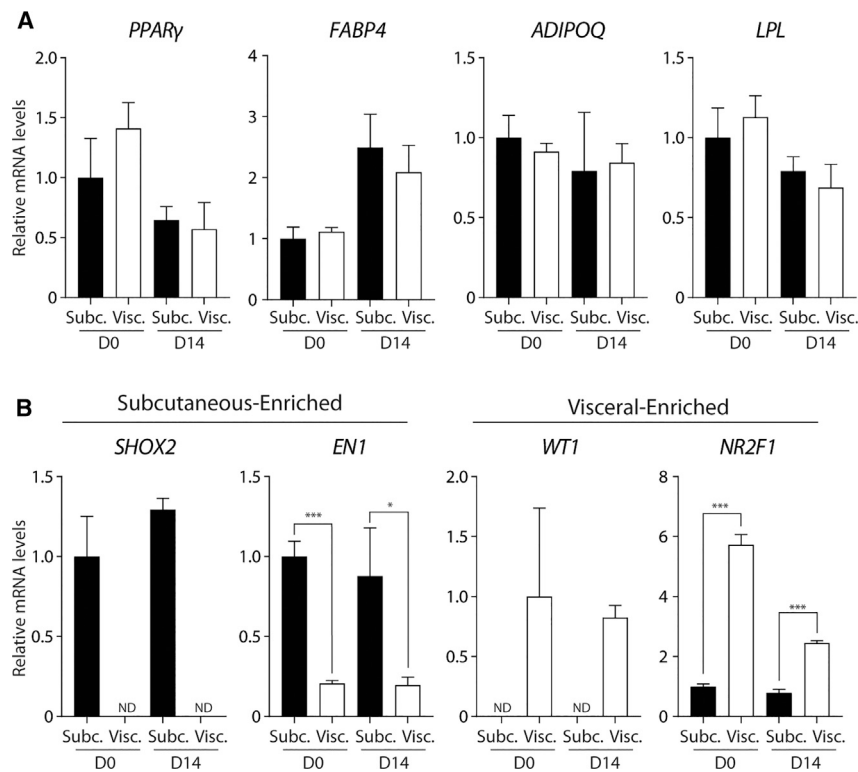


**Figure 3. Human MAAC Maintain Their Depot-Specific Gene Expression Patterns**

(A) mRNA levels of adipogenic genes in human subcutaneous (subc.) and omental visceral (visc.) adipocytes freshly isolated (D0) and cultured under a membrane for 2 weeks (D14) (mean  $\pm$  SD, n = 3). (B) mRNA levels of subcutaneous and visceral-enriched genes in human subcutaneous and visceral adipocytes freshly isolated (D0) and cultured under a membrane for 2 weeks (D14) (mean  $\pm$  SD, n = 3). \*p < 0.05; \*\*p < 0.01; \*\*\*p < 0.001

adipocytes, and *NR2F1* was expressed almost 6-fold higher in visceral adipocytes relative to subcutaneous adipocytes. After 2 weeks of culture under membranes, the differential expression of these visceral adipocyte-enriched genes was also conserved.

This was also true for murine adipocytes. Similar to subcutaneous adipocytes, visceral adipocytes from the epididymal depot of 8-week-old CD1 female mice cultured under a membrane for 1 week maintained normal expression of *PPAR $\gamma$* , *Fabp4*, *Lipe*, and *Lpl* (Figure S3A). *Shox2* and *En1* were enriched in subcutaneous adipocytes and maintained a depot-specific expression pattern for 1 week of culture (Figure S3B). *Wt1* and *Nr2f1* were enriched in visceral adipocytes; however, only *Wt1* conserved a statistical difference. Together, these results indicate that membrane-cultured adipocytes maintain depot-specific expression patterns *in vitro*.

### MAAC Remain Functional and Have Improved Translational Relevance

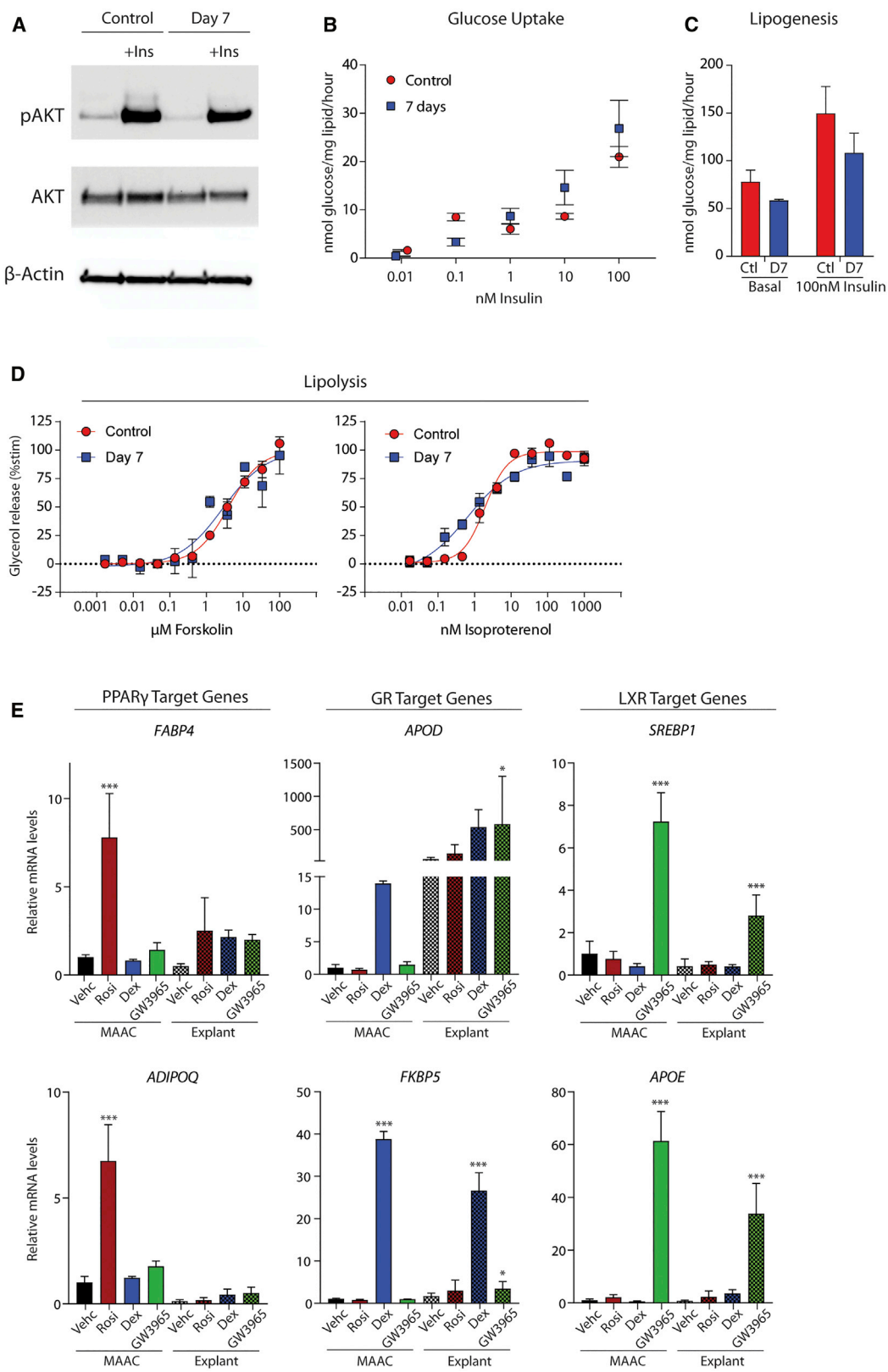
A key function of adipocytes is to maintain systemic energy balance by storing glucose and fatty acids postprandially when insulin levels are high and undergoing lipolysis during fasting (Rosen and Spiegelman, 2014). MAAC cultured for 7 days remained fully functional and maintained normal insulin sensitivity, as evidenced by the robust increase in AKT phosphorylation following insulin stimulation, which was similar to the response observed in isolated mature adipocytes allowed to recover overnight following collagenase digestion of the tissue (Figure 4A). Insulin stimulated glucose-uptake was maintained in MAAC after 7 days of culture, which displayed a dose-dependent increase in glucose uptake similar to levels measured in control adipo-

cytes (Figure 4B). Basal and insulin-stimulated *de novo* lipogenesis was also preserved after 7 days of culture relative to control adipocytes (Figure 4C), as was lipolytic response to catecholamines (Figure 4D). Of note, basal lipolysis of MAAC cultured for 1 week was increased by a modest 15% (Figure S4A), which is much lower than the reported increase for the explant model (Gesta et al., 2003), and basal lipogenesis was decreased by ~25% (Figure 4D).

To determine whether MAAC could respond appropriately to diverse pharmacological stimuli, explants and MAAC

were treated with the PPAR $\gamma$  agonist rosiglitazone (Rosi), the glucocorticoid receptor (GR) agonist dexamethasone, or the liver X receptor (LXR) agonist GW3965 for 7 days, and the expression of canonical PPAR $\gamma$ , GR, and LXR responsive genes were measured. The explants were generally unable to respond or responded in an inconsistent manner, whereas the membrane-cultured cells responded in a robust and highly specific manner. Specifically, Rosi drove the expression of *FABP4*, *ADIPOQ*, *PCK1*, and *LPL* by 4- to 12-fold in MAAC compared to untreated cells, whereas neither dexamethasone nor GW3965 had an effect on these PPAR $\gamma$  target genes (Figures 4E and S4B). By contrast, Rosi modestly increased the expression of *FABP4* but none of the other PPAR $\gamma$  target genes in the adipose tissue explants. Similarly, in MAAC, dexamethasone increased the expression of the GR target genes *APOD* and *FKBP5* by 15- and 40-fold, respectively, whereas in the explants, all chemicals, including the PPAR $\gamma$  and LXR agonists, increased the expression of *APOD* 3- to 11-fold. GW3965 increased the expression of the LXR target gene *SREBP1* by 7-fold and *APOE* by ~50-fold in both MAAC and explants.

One inherent benefit of using a membrane is the ability to co-culture different cell types. Cells from the mouse macrophage cell line RAW264 were placed on top of the membrane and were co-cultured with MAAC. The co-cultures were treated with or without lipopolysaccharide (LPS) for 18 hours to trigger an inflammatory response, after which the medium was collected and analyzed. We leveraged the species difference by using human or mouse-specific ELISAs to determine how the different cell types responded. Mature adipocytes treated with LPS in the absence of macrophages responded



(legend on next page)

by increasing interleukin-6 (IL-6) and IL-8 protein secretion by 10- and 30-fold, respectively (Figure 5A). Interestingly, when adipocytes were co-cultured with macrophages, human IL-6 and IL-8 protein levels in the medium further increased by approximately 6-fold, indicating a synergistic regulation. This was not observed for all cytokines, as the LPS-induced secretion of tumor necrosis factor alpha (TNF $\alpha$ ), interferon gamma (IFN $\gamma$ ), IL-1B, and IL-12P70 from human adipocytes was only modestly increased when co-cultured with macrophages (Figure S5A). We next quantified cytokines in the medium using a mouse-specific ELISA to measure the response from the murine macrophages to LPS and whether these cytokines could be affecting the human adipocytes. LPS drove a massive 1,500-fold increase in murine TNF $\alpha$  protein levels but more modest increases in IL-6, IL-1B, KC (IL-8), IL-12P70, and IL-10 (Figure 5B; Figure S5B). Interestingly, we found that co-culture with adipocytes further increased the levels of TNF $\alpha$  produced by macrophages by 50% and IL-6 by 100%. Conditioned medium from LPS-treated macrophages was added to MAAC, elevating IL-6 and IL-8 protein levels 35- and 70-fold, respectively (Figure 5C). The addition of a neutralizing TNF $\alpha$  antibody to the conditioned medium led to a dose-dependent decrease in human IL-6 and IL-8 protein levels, indicating that macrophage-derived TNF $\alpha$  promotes a synergistic increase in IL-6 and IL-8 production in human adipocytes. Together, these results indicate that the MAAC were fully functional and capable of engaging in signaling and crosstalk with another cell type.

#### Mature Human White Adipocytes Can Transdifferentiate into Brown-like Adipocytes

The appearance of thermogenic brown-like adipocytes in white adipose tissues occurs in animals under specific stimuli, such as cold exposure. Lineage-tracing studies in mice have revealed that these UCP1+ adipocytes arise from *de novo* differentiation of precursors, but others have suggested that transdifferentiation from mature adipocytes may also occur, depending on the browning stimulus used (Jeremic et al., 2017; Jiang et al., 2017; Vitali et al., 2012). It is now clear that humans possess significant amounts of brown fat within cervical, supraclavicular, paraspinal, and abdominal adipose depots (Leitner et al., 2017). However, it is unknown whether mature human white adipocytes can transdifferentiate into brown-like fat cells.

We transduced human MAAC with adenovirus-encoding GFP, which resulted in high levels of GFP fluorescence in most adipocytes, indicating that mature adipocytes are effectively transduced and that MAAC can be used for gain- or loss-of-function experiments (Figure 6A). Transduction of mature human subcutaneous white adipocytes with adenovirus-containing *PGC1 $\alpha$* , the master regulator of mitochondrial biogenesis, resulted in a

robust overexpression of *PGC1 $\alpha$*  (Figures 6B and 6D), which drove a broad brown fat transcriptional program, including a 15-fold induction of *UCP1* and *CIDEA* and over a 200-fold induction of *PPAR $\alpha$*  and *EBF2*, 7 days after transduction (Figure 6C). Importantly, the UCP1 protein was also increased, indicating that mature human subcutaneous white adipocytes are competent to transdifferentiate into brown-like adipocytes (Figure 6D). We also tested the browning potential of FGF21, BMP7, BMP4, Irisin, Rosi, and T<sub>3</sub> in mature human subcutaneous adipocytes and found that a 7-day treatment of adipocytes with Rosi and T<sub>3</sub> caused a 25-fold and 3.5-fold increase in *UCP1* mRNA, respectively, whereas the other molecules had no effect. Of note, none of the stimuli caused an increase in *UCP1* in adipose tissue explants (Figure 6E). Interestingly, we found that the addition of insulin in the culture medium was required for Rosi-induced *UCP1* upregulation (Figure 6F). By contrast, insulin was not required for *PGC1 $\alpha$* -mediated *UCP1* induction, although it further increased *UCP1* levels 2-fold (Figure 6G). Together, these results indicate that MAAC can be used to study long-term adipocyte phenotypic changes and that mature human subcutaneous white adipocytes have the potential to transdifferentiate into brown-like adipocytes.

#### DISCUSSION

The development of efficacious drugs that act on adipocytes for the treatment of diabetes and obesity requires relevant translational *in vitro* models. However, current methods to study adipocyte biology all have limitations. We confirmed that adipocytes cultured on the ceiling of a flask rapidly dedifferentiate and lose all their lipids (Figures 1C and S1C), as previously reported (Adebonojo, 1975; Asada et al., 2011; Lessard et al., 2015; Shen et al., 2011; Sugihara et al., 1989; Wei et al., 2013). Similarly, culture of small adipose tissue pieces (explants) rapidly lose their adipogenic gene signature (Figures 1C, 2A, and S2C) (Fain et al., 2010; Gesta et al., 2003). We also showed that explants do not respond appropriately to PPAR $\gamma$  and GR agonism, indicating that these pathways are not maintained in this model and that this model is not suitable for all applications and questions. Interestingly, primary human preadipocytes differentiated *in vitro* possess an adipogenic gene signature very similar to freshly isolated human adipocytes and adipose tissue, confirming that they are a useful model for studying adipocyte function and the process of differentiation in particular. However, unbiased RNA-seq analysis reveals that globally, their gene expression signature remains quite different from a true adipocyte. This is particularly evident when looking at the morphology of these cells (Figure 2B), which remain quite small (diameter, <35  $\mu$ m) and possess multilocular lipid droplets, compared to a normal unilocular lipid

#### Figure 4. Human Membrane-Cultured Adipocytes Remain Functional

- (A) Western blot analysis of pAKT, AKT, and  $\beta$ -actin after a 10-minute insulin stimulation, comparing adipocytes that recovered under membranes overnight (control) or cultured for 7 days.
- (B) Basal and insulin-stimulated glucose uptake in MAAC that recovered under membranes overnight (control) or cultured for 7 days (mean  $\pm$  SD, n = 4).
- (C) Basal and insulin-stimulated *de novo* lipogenesis of MAAC that recovered under membranes overnight (Ctl) or cultured for 7 days (D7) (mean  $\pm$  SD, n = 4).
- (D) Basal and forskolin- and isoproterenol-stimulated lipolysis in adipocytes cultured under membranes overnight (control) or for 7 days; (mean  $\pm$  SD, n = 4).
- (E) mRNA analysis of PPAR $\gamma$ , glucocorticoid receptor (GR), and liver X receptor (LXR) target genes in MAAC and explants after 7 days of culture in the presence of 10  $\mu$ M of the PPAR $\gamma$  agonist rosiglitazone (Rosi), GR agonist dexamethasone (Dex), or LXR agonist GW3965 (mean  $\pm$  SD, n = 4). \*p < 0.05; \*\*p < 0.01; \*\*\*p < 0.001

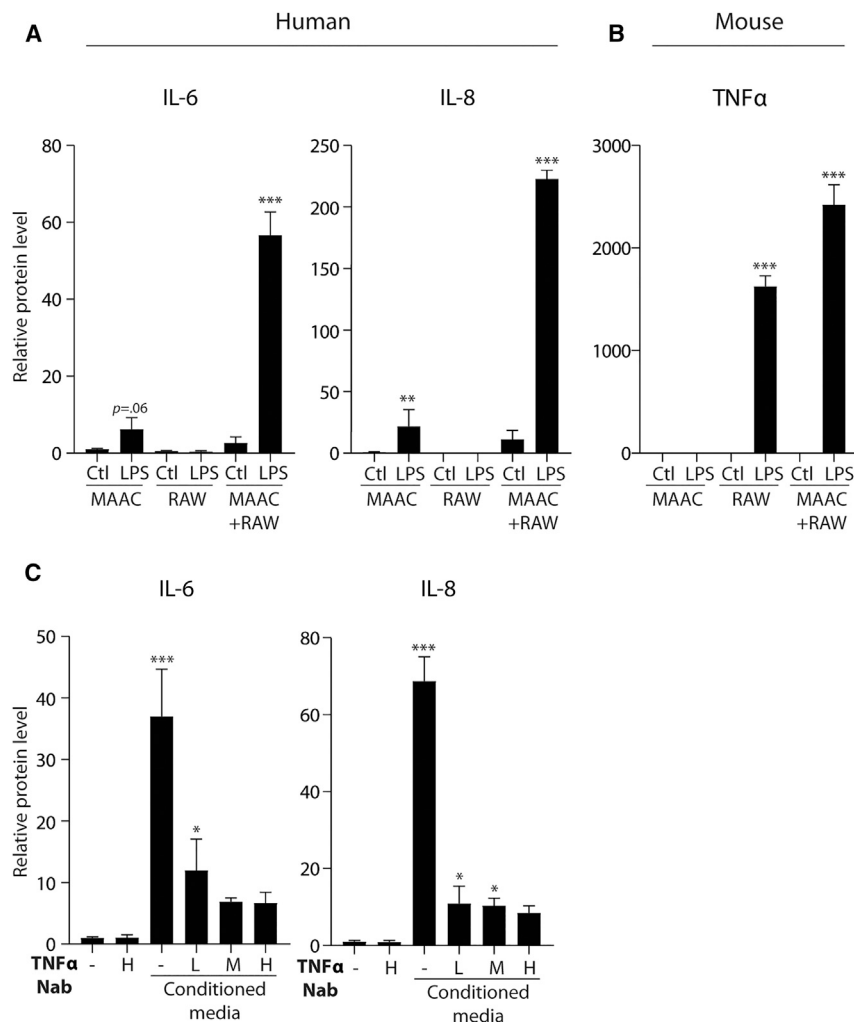


**Figure 5. MAAC Can Crosstalk with Macrophages**

(A and B) Human IL-6 and IL-8 protein levels (A) and mouse TNF $\alpha$  protein levels (B) in the culture medium of human adipocytes, mouse macrophages, or adipocyte + macrophage co-cultures treated with vehicle (Ctl) or 10 ng/ml of LPS for 18 hours (mean  $\pm$  SD, n = 4).

(C) Human IL-6 and IL-8 protein levels in the culture medium of human adipocytes treated with conditioned medium from mouse macrophages that had been cultured with 10 ng/ml of LPS for 18 hours and/or neutralizing TNF $\alpha$  antibody (mean  $\pm$  SD, n = 3). \*p < 0.05; \*\*p < 0.01; \*\*\*p < 0.001

touted for their ability to allow oxygen and nutrients to diffuse, as well as a decreased elastic modulus (rigidity) relative to standard tissue culture plastic (Arjun and Ramesh, 2012; Callister and Callister, 2001; Shamir and Ewald, 2014). We believe that there are multiple factors that play a role in preserving MAAC identity and function. Matrix stiffness is well known to impact many processes, including adipogenesis, cell lineage specificity, dictating cellular behavior, and disease progression (Cristancho and Lazar, 2011; Engler et al., 2006; Handorf et al., 2015; Shoham and Gefen, 2012). When the adipocytes are pipetted onto the membrane, the material that the adipocytes are in contact with is approximately 100-fold less rigid than standard tissue culture plastic (Arjun and Ramesh, 2012; Callister and Callister, 2001). Moreover, only a monolayer of less than 10%

droplet containing white adipocyte with an average diameter of 100  $\mu$ m. Furthermore, *in-vitro*-differentiated adipocytes, in particular from mouse, undergo a loss of phenotype when cultured for a long time (Kuri-Harcuch and Green, 1977; Wise and Green, 1978).

Here, we have developed a method for culturing freshly isolated mature adipocytes under permeable membranes. This method presents numerous advances and advantages over existing techniques. We start from physiologically relevant, patient-derived cells that do not require differentiation with an unphysiological chemical cocktail. Even after 2 weeks in culture, unbiased RNA-seq analysis revealed that the gene expression profile of MAAC is the closest to the starting adipocytes, relative to other methods. MAAC retain depot-specific expression patterns and functionally respond to diverse physiologic cues. Furthermore, because the mature cells are fully differentiated, one can treat the cells or perform gain- or loss-of-function experiments without impacting the differentiation process, which can be a confounding factor when performing experiments in differentiating preadipocytes.

Permeable membranes have been used for biologic research for over 65 years (Grobstein, 1953). They are widely

of the adipocytes interact with the membrane, and most of the adipocytes are stacked on top of each other in a 3D aggregate culture. In this way, the cells maintain key cell-cell contacts, and the elastic modulus that most cells encounter is that of adipose, which is 2 KPa relative to the 1GPa of standard cultures (Skardal et al., 2013), a fold difference of 500,000.

In addition, we showed that hypoxia acutely drives a loss of adipogenic gene expression (Figure S1E). Thus, at normoxia, the porous membrane may help to improve oxygen access and maintain the expression of adipogenic genes in MAAC (Shamir and Ewald, 2014), mitigating hypoxic stress that is a well-known driver of phenotypic change in adipose tissue (Gesta et al., 2003; Sun et al., 2011; Trayhurn, 2013, 2014). Indeed, MAAC are under reduced hypoxic stress compared to explants, where passive diffusion of oxygen and nutrients appears to be limiting, at least under our experimental conditions (Figure 1E). It is possible that explant models could be improved by adding flow and incorporating microfluidic pumps or agitation, as has benefitted other models (Dehne et al., 2017). Recent years have seen a push to develop microphysiological systems

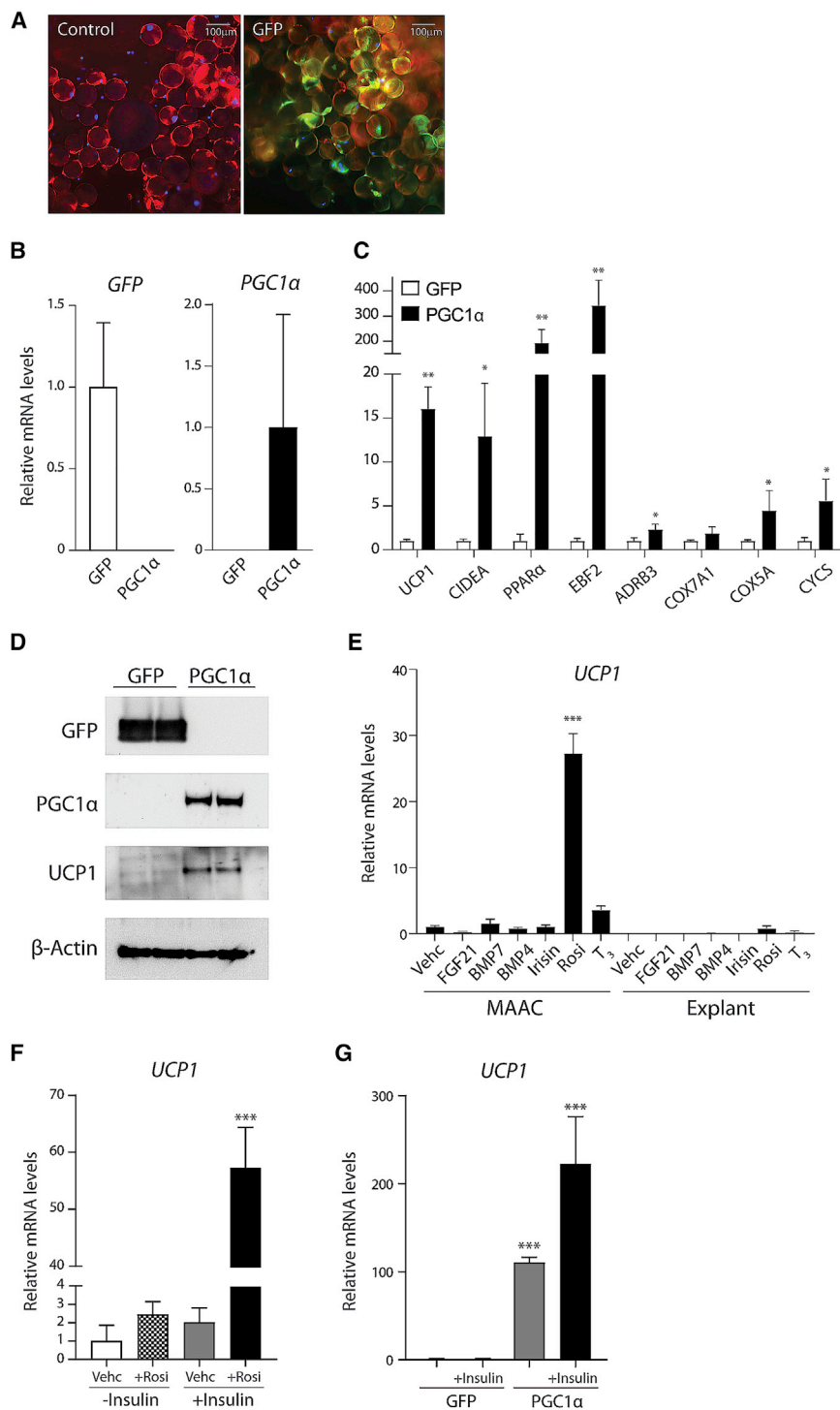


**Figure 6. MAAC Can Transdifferentiate into Brown-like Adipocytes**

(A) Images comparing control MAAC and MAAC that were transduced with adenovirus encoding GFP after 72 hours. Blue, Hoechst 33342 (nuclei); red, cell mask deep red (plasma membrane); green, GFP.

(B) mRNA levels of *GFP* and *PGC1α* in MAAC, 7 days after transduction with adenovirus encoding *GFP* or *PGC1α* (mean  $\pm$  SD, n = 4).

(C) mRNA levels of brown fat-enriched genes in MAAC 7 days after transduction with adenovirus encoding *GFP* or *PGC1α* (mean  $\pm$  SD, n = 4).

(D) Western blot analysis of *GFP*, *PGC1α*, *UCP1*, and  $\beta$ -actin in MAAC 7 days after transduction with adenovirus encoding *GFP* or *PGC1α*.

(E) mRNA levels of *UCP1* in MAAC and explants treated with FGF21, BMP7, BMP4, Irisin, Rosi, or T<sub>3</sub> for 7 days (mean  $\pm$  SD, n = 3).

(F) mRNA levels of *UCP1* in MAAC 7 days after treatment with or without insulin and Rosi (mean  $\pm$  SD, n = 3).

(G) mRNA levels of *UCP1* in MAAC 7 days after transduction with adenovirus encoding *GFP* or *PGC1α* and treatment with or without insulin (mean  $\pm$  SD, n = 4). \*p < 0.05; \*\*p < 0.01; \*\*\*p < 0.001

(Wikswow, 2014). Moreover, for adipose research, current MPS are built for differentiated preadipocytes and do not accommodate mature adipocytes (Loskill et al., 2017; Wu et al., 2016).

Enriched gene ontology (GO) terms of DEGs from MAAC, floating adipocytes, and differentiated preadipocytes revealed specific changes that occur in the respective models. In particular, we found that differentiated precursors had a striking decrease in the expression of genes associated with cell morphology (Figure S2D). Among the genes involved in cell morphogenesis, we found 18 in the adipose-enriched signature that showed an overall decreased expression in differentiated preadipocytes and higher levels in adipose tissue, D0 adipocytes, and MAAC (Figure S2E). Interestingly, this list of genes contains many developmental factors known to impact differentiation and substrate handling, suggesting that the decreased expression of one or more of these genes may

(MPS) to better mimic *in vivo* environments *in vitro* (Dehne et al., 2017; Wikswow, 2014). MPS or “organs-on-chips” use pumps and tubing to link culture chambers containing different cell types. However, many limitations exist for these systems including: low throughput, high cost, and technical issues related to small volumes and sample sizes that still require resolving

explain the multilocular morphology found in differentiated preadipocytes. For example, *TNMD*, a factor known to be required for differentiation (Senol-Cosar et al., 2016), had 16-fold lower levels in differentiated preadipocytes than the control adipocytes.

Even though the RNA-seq data showed that the MAAC gene expression profile is most similar to control adipocytes relative

to other models, all models, including MAAC, have high numbers of DEGs. Given the well-documented changes that occur to adipocytes upon isolation by collagenase digestion, many changes may be attributable to the temporary changes occurring in the control adipocytes (Ruan et al., 2003). The RNA-seq data also indicate that floating human adipocytes without membrane support maintain a gene expression profile relatively similar to starting material, albeit performing worse than MAAC. Because this method does not require the purchase of permeable membranes, perhaps it can be utilized in experiments where coarser models are sufficient or relatively short treatment times are needed. Mouse adipocytes, however, have a rapid drop off in gene expression after 3 days when cultured without membrane support. Under membranes, mouse adipocytes eventually start losing their adipocyte gene signature when cultured for extended lengths of time. Thus, we do not recommend culturing murine adipocytes without membrane support and for no longer than 1 week. Additionally, as mouse adipocytes are more fragile than human adipocytes, we found that a short time of digestion of adipose tissue with collagenase and using young mice are recommended for culture of mouse adipocyte under membranes.

One often overlooked challenge facing the adipose field is a lack of *in vitro* models for visceral adipocytes. Visceral, rather than subcutaneous fat, is thought to contribute more to insulin resistance and the metabolic syndrome (Rosen and Spiegelman, 2014; Tran and Kahn, 2010). The culture of visceral preadipocytes has been notoriously challenging (Macotela et al., 2012); thus, almost all primary cell models rely on isolating precursors from subcutaneous fat. Here, we have shown that we can culture subcutaneous and visceral adipocytes from both human and mouse and they maintain their unique depot-specific gene expression patterns. Therefore, the membrane culture system is a unique method to study mature visceral adipocytes, which can facilitate the future study of differences between subcutaneous and visceral adipocytes from lean or obese patients with different metabolic profiles.

An additional advantage to using a membrane is the ability to co-culture other cell types with mature adipocytes. We showed that it is possible to observe the crosstalk between adipocytes and macrophages. Given the profound role that the immune system can play in insulin resistance (Brestoff and Artis, 2015; Lee et al., 2018; Odegaard and Chawla, 2013; Saltiel and Olefsky, 2017), these results have far reaching implications that can help the study of adipocyte interaction with the immune system, immune cell recruitment, and activation by adipocytes, as well as facilitate the development of anti-inflammatory drugs for the treatment of insulin resistance. Moreover, future experiments can be performed to study the influence of adipocytes on other cell types, including preadipocytes, endothelial cells, pancreatic islets, and hepatocytes.

Human preadipocytes differentiated *in vitro* have been shown to be able to acquire brown-like features following treatment with Rosi or other PPAR $\gamma$ -related compounds (Hondares et al., 2011; Loft et al., 2015) or overexpression of PGC1 $\alpha$  (Tiraby et al., 2003). Here, we provide direct evidence that mature human white adipocytes can transdifferentiate into brown-like adipocytes. Both overexpression of PGC1 $\alpha$  and Rosi treatment robustly increase *UCP1* levels. Interestingly, it has been postu-

lated that only certain adipose tissue depots are capable of browning in human and that the subcutaneous adipose tissue depot cannot (Leitner et al., 2017). Here, we used mature human subcutaneous adipocytes and demonstrated that browning is possible, suggesting that it may be feasible to pharmacologically convert human subcutaneous and other white adipocytes into brown-like adipocytes for the treatment of T2D and obesity. However, it is unclear if we captured the full browning potential of the cells. It remains unknown if the PGC1 $\alpha$  virus transduced all cells and whether all subcutaneous adipocytes have the potential to transdifferentiate or if only a subpopulation have that capacity. Interestingly, we found that the addition of insulin in the culture medium was required for Rosi but not PGC1 $\alpha$ -mediated *UCP1* induction, suggesting that PPAR $\gamma$  and insulin signaling have synergistic effects upstream of PGC1 $\alpha$ .

Lastly, the membranes used are available in multiwell formats, making them a viable model for drug screening. Taken together, MAAC is a culture method allowing the study of long-term phenotypic changes of adipocytes, allowing crosstalk between adipocytes and other cell types, and provides an improved translational model for drug development and the modulation of adipose tissue function.

## STAR★METHODS

Detailed methods are provided in the online version of this paper and include the following:

- KEY RESOURCES TABLE
- CONTACT FOR REAGENT AND RESOURCE SHARING
- EXPERIMENTAL MODEL AND SUBJECT DETAILS
  - Animals
  - Human adipose
  - Cell Lines
- METHOD DETAILS
  - Mouse adipose
  - Human adipose
  - Membrane Setup
  - Preadipocyte Isolation and differentiation
  - Cell Culture
  - Real-Time PCR and Western Blot Analysis
  - Functional Assays
  - Co-Culture
  - Imaging
  - RNA-Sequencing
  - Bioinformatics
- QUANTIFICATION AND STATISTICAL ANALYSIS
- DATA AND SOFTWARE AVAILABILITY

## SUPPLEMENTAL INFORMATION

Supplemental Information can be found online at <https://doi.org/10.1016/j.celrep.2019.03.026>.

## ACKNOWLEDGMENTS

M.J.H. is a fellow of the AstraZeneca postdoc program. A.T. was supported by the Erling-Persson Family Foundation. C.E.H. was supported by the Swedish

Society for Medical Research (SSMF) and by Karolinska Institutet. A.M. and J.B. were supported by the Knut and Alice Wallenberg Foundation. This study was supported by grants from the European Research Council (Starting Investigator Grant No. 261258 to K.L.S.), the Swedish Research Council, the Vallee Foundation and the Diabetes Research Program and Karolinska Institutet.

## AUTHOR CONTRIBUTIONS

Conceptualization, M.J.H. and J.B.; Methodology, M.J.H.; Validation, Q.L.; Formal Analysis, S.L. and C.Z.; Investigation, M.J.H., Q.L., B.K., S.H., I.A., and C.E.H.; Resources, A.T. and X.P.; Writing – Original Draft, M.J.H. and J.B.; Writing – Review and Editing, all authors; Supervision, A.M., K.L.S. and J.B.

## DECLARATION OF INTERESTS

The authors declare no competing interests.

Received: June 13, 2018  
Revised: January 23, 2019  
Accepted: March 6, 2019  
Published: April 2, 2019

## REFERENCES

- Adebonojo, F.O. (1975). Studies on human adipose cells in culture: relation of cell size and multiplication to donor age. *Yale J. Biol. Med.* **48**, 9–16.
- Ahmadian, M., Suh, J.M., Hah, N., Liddle, C., Atkins, A.R., Downes, M., and Evans, R.M. (2013). PPAR $\gamma$  signaling and metabolism: the good, the bad and the future. *Nat. Med.* **19**, 557–566.
- Anders, S., and Huber, W. (2010). Differential expression analysis for sequence count data. *Genome Biol.* **11**, R106.
- Arjun, G.N., and Ramesh, P. (2012). Structural characterization, mechanical properties, and in vitro cytocompatibility evaluation of fibrous polycarbonate urethane membranes for biomedical applications. *J. Biomed. Mater. Res. A* **100**, 3042–3050.
- Asada, S., Kuroda, M., Aoyagi, Y., Fukaya, Y., Tanaka, S., Konno, S., Tanio, M., Aso, M., Satoh, K., Okamoto, Y., et al. (2011). Ceiling culture-derived proliferative adipocytes retain high adipogenic potential suitable for use as a vehicle for gene transduction therapy. *Am. J. Physiol. Cell Physiol.* **307**, C181–C185.
- Brestoff, J.R., and Artis, D. (2015). Immune regulation of metabolic homeostasis in health and disease. *Cell* **161**, 146–160.
- Callister, W.D., and Callister, W.D. (2001). *Fundamentals of materials science and engineering: an interactive text* (Wiley).
- Cristancho, A.G., and Lazar, M.A. (2011). Forming functional fat: a growing understanding of adipocyte differentiation. *Nat. Rev. Mol. Cell Biol.* **12**, 722–734.
- Dehne, E.M., Hasenberg, T., and Marx, U. (2017). The ascendance of microphysiological systems to solve the drug testing dilemma. *Future Sci. OA* **3**, FSO185.
- Engler, A.J., Sen, S., Sweeney, H.L., and Discher, D.E. (2006). Matrix elasticity directs stem cell lineage specification. *Cell* **126**, 677–689.
- Fain, J.N., Cheema, P., Madan, A.K., and Tichansky, D.S. (2010). Dexamethasone and the inflammatory response in explants of human omental adipose tissue. *Mol. Cell. Endocrinol.* **315**, 292–298.
- Fresno, C., and Fernández, E.A. (2013). RDAVIDWebService: a versatile R interface to DAVID. *Bioinformatics* **29**, 2810–2811.
- Gesta, S., Lolmede, K., Daviaud, D., Berlan, M., Bouloumie, A., Lafontan, M., Valet, P., and Saulnier-Blache, J.S. (2003). Culture of human adipose tissue explants leads to profound alteration of adipocyte gene expression. *Horm. Metab. Res.* **35**, 158–163.
- Gesta, S., Blüher, M., Yamamoto, Y., Norris, A.W., Berndt, J., Kralisch, S., Boucher, J., Lewis, C., and Kahn, C.R. (2006). Evidence for a role of developmental genes in the origin of obesity and body fat distribution. *Proc. Natl. Acad. Sci. USA* **103**, 6676–6681.
- Gregoire, F.M., Smas, C.M., and Sul, H.S. (1998). Understanding adipocyte differentiation. *Physiol. Rev.* **78**, 783–809.
- Grobstein, C. (1953). Morphogenetic interaction between embryonic mouse tissues separated by a membrane filter. *Nature* **172**, 869–870.
- Guilherme, A., Virbasius, J.V., Puri, V., and Czech, M.P. (2008). Adipocyte dysfunctions linking obesity to insulin resistance and type 2 diabetes. *Nat. Rev. Mol. Cell Biol.* **9**, 367–377.
- Handorf, A.M., Zhou, Y., Halanski, M.A., and Li, W.J. (2015). Tissue stiffness dictates development, homeostasis, and disease progression. *Organogenesis* **11**, 1–15.
- Harms, M., and Seale, P. (2013). Brown and beige fat: development, function and therapeutic potential. *Nat. Med.* **19**, 1252–1263.
- Hondares, E., Rosell, M., Díaz-Delfín, J., Olmos, Y., Monsalve, M., Iglesias, R., Villarroya, F., and Giralt, M. (2011). Peroxisome proliferator-activated receptor  $\alpha$  (PPAR $\alpha$ ) induces PPAR $\gamma$  coactivator 1 $\alpha$  (PGC-1 $\alpha$ ) gene expression and contributes to thermogenic activation of brown fat: involvement of PRDM16. *J. Biol. Chem.* **286**, 43112–43122.
- Huang, W., Sherman, B.T., and Lempicki, R.A. (2009). Bioinformatics enrichment tools: paths toward the comprehensive functional analysis of large gene lists. *Nucleic Acids Res.* **37**, 1–13.
- Jeremic, N., Chaturvedi, P., and Tyagi, S.C. (2017). Browning of White Fat: Novel Insight Into Factors, Mechanisms, and Therapeutics. *J. Cell. Physiol.* **232**, 61–68.
- Jiang, Y., Berry, D.C., and Graff, J.M. (2017). Distinct cellular and molecular mechanisms for  $\beta$ 3 adrenergic receptor-induced beige adipocyte formation. *eLife* **6**, e30329.
- Kim, D., Langmead, B., and Salzberg, S.L. (2015). HISAT: a fast spliced aligner with low memory requirements. *Nat. Methods* **12**, 357–360.
- Kuri-Harcuch, W., and Green, H. (1977). Increasing activity of enzymes on pathway of triacylglycerol synthesis during adipose conversion of 3T3 cells. *J. Biol. Chem.* **252**, 2158–2160.
- Lee, Y.S., Wollam, J., and Olefsky, J.M. (2018). An Integrated View of Immunometabolism. *Cell* **172**, 22–40.
- Leitner, B.P., Huang, S., Brychta, R.J., Duckworth, C.J., Baskin, A.S., McGehee, S., Tal, I., Dieckmann, W., Gupta, G., Kolodny, G.M., et al. (2017). Mapping of human brown adipose tissue in lean and obese young men. *Proc. Natl. Acad. Sci. USA* **114**, 8649–8654.
- Lessard, J., Pelletier, M., Biertho, L., Biron, S., Marceau, S., Hould, F.S., Lebel, S., Moustarah, F., Lescelleur, O., Marceau, P., and Tchernof, A. (2015). Characterization of dedifferentiating human mature adipocytes from the visceral and subcutaneous fat compartments: fibroblast-activation protein alpha and dipeptidyl peptidase 4 as major components of matrix remodeling. *PLoS One* **10**, e0122065.
- Loft, A., Forss, I., Siersbæk, M.S., Schmidt, S.F., Larsen, A.S., Madsen, J.G., Pisani, D.F., Nielsen, R., Aagaard, M.M., Mathison, A., et al. (2015). Browning of human adipocytes requires KLF11 and reprogramming of PPAR $\gamma$  superenhancers. *Genes Dev.* **29**, 7–22.
- Loskill, P., Sezhian, T., Tharp, K.M., Lee-Montiel, F.T., Jeeawoody, S., Reese, W.M., Zushin, P.H., Stahl, A., and Healy, K.E. (2017). WAT-on-a-chip: a physiologically relevant microfluidic system incorporating white adipose tissue. *Lab Chip* **17**, 1645–1654.
- Lotta, L.A., Gulati, P., Day, F.R., Payne, F., Ongen, H., van de Bunt, M., Gaulton, K.J., Eicher, J.D., Sharp, S.J., Luan, J., et al.; EPIC-InterAct Consortium; Cambridge FPLD1 Consortium (2017). Integrative genomic analysis implicates limited peripheral adipose storage capacity in the pathogenesis of human insulin resistance. *Nat. Genet.* **49**, 17–26.
- Macotela, Y., Emanuelli, B., Mori, M.A., Gesta, S., Schulz, T.J., Tseng, Y.H., and Kahn, C.R. (2012). Intrinsic differences in adipocyte precursor cells from different white fat depots. *Diabetes* **61**, 1691–1699.
- McBeath, R., Pirone, D.M., Nelson, C.M., Bhadriraju, K., and Chen, C.S. (2004). Cell shape, cytoskeletal tension, and RhoA regulate stem cell lineage commitment. *Dev. Cell* **6**, 483–495.

- Merico, D., Isserlin, R., Stueker, O., Emili, A., and Bader, G.D. (2010). Enrichment map: a network-based method for gene-set enrichment visualization and interpretation. *PLoS One* 5, e13984.
- Odegaard, J.I., and Chawla, A. (2013). Pleiotropic actions of insulin resistance and inflammation in metabolic homeostasis. *Science* 339, 172–177.
- Patro, R., Mount, S.M., and Kingsford, C. (2014). Sailfish enables alignment-free isoform quantification from RNA-seq reads using lightweight algorithms. *Nat. Biotechnol.* 32, 462–464.
- Rosen, E.D., and MacDougald, O.A. (2006). Adipocyte differentiation from the inside out. *Nat. Rev. Mol. Cell Biol.* 7, 885–896.
- Rosen, E.D., and Spiegelman, B.M. (2014). What we talk about when we talk about fat. *Cell* 156, 20–44.
- Ruan, H., Zarnowski, M.J., Cushman, S.W., and Lodish, H.F. (2003). Standard isolation of primary adipose cells from mouse epididymal fat pads induces inflammatory mediators and down-regulates adipocyte genes. *J. Biol. Chem.* 278, 47585–47593.
- Ruiz-Ojeda, F.J., Rupérez, A.I., Gomez-Llorente, C., Gil, A., and Aguilera, C.M. (2016). Cell Models and Their Application for Studying Adipogenic Differentiation in Relation to Obesity: A Review. *Int. J. Mol. Sci.* 17, E1040.
- Saltiel, A.R., and Olefsky, J.M. (2017). Inflammatory mechanisms linking obesity and metabolic disease. *J. Clin. Invest.* 127, 1–4.
- Samuel, V.T., and Shulman, G.I. (2012). Mechanisms for insulin resistance: common threads and missing links. *Cell* 148, 852–871.
- Sarjeant, K., and Stephens, J.M. (2012). Adipogenesis. *Cold Spring Harb. Perspect. Biol.* 4, a008417.
- Senol-Cosar, O., Flach, R.J., DiStefano, M., Chawla, A., Nicoloso, S., Straubhaar, J., Hardy, O.T., Noh, H.L., Kim, J.K., Wabitsch, M., et al. (2016). Tenomodulin promotes human adipocyte differentiation and beneficial visceral adipose tissue expansion. *Nat. Commun.* 7, 10686.
- Shamir, E.R., and Ewald, A.J. (2014). Three-dimensional organotypic culture: experimental models of mammalian biology and disease. *Nat. Rev. Mol. Cell Biol.* 15, 647–664.
- Shen, J.F., Sugawara, A., Yamashita, J., Ogura, H., and Sato, S. (2011). Dedifferentiated fat cells: an alternative source of adult multipotent cells from the adipose tissues. *Int. J. Oral Sci.* 3, 117–124.
- Shoham, N., and Gefen, A. (2012). Mechanotransduction in adipocytes. *J. Biomech.* 45, 1–8.
- Siersbæk, R., Nielsen, R., and Mandrup, S. (2012). Transcriptional networks and chromatin remodeling controlling adipogenesis. *Trends Endocrinol. Metab.* 23, 56–64.
- Skardal, A., Mack, D., Atala, A., and Soker, S. (2013). Substrate elasticity controls cell proliferation, surface marker expression and motile phenotype in amniotic fluid-derived stem cells. *J. Mech. Behav. Biomed. Mater.* 17, 307–316.
- Sugihara, H., Yonemitsu, N., Miyabara, S., and Yun, K. (1986). Primary cultures of unilocular fat cells: characteristics of growth in vitro and changes in differentiation properties. *Differentiation* 31, 42–49.
- Sugihara, H., Yonemitsu, N., Miyabara, S., and Toda, S. (1987). Proliferation of unilocular fat cells in the primary culture. *J. Lipid Res.* 28, 1038–1045.
- Sugihara, H., Funatsumaru, S., Yonemitsu, N., Miyabara, S., Toda, S., and Hikiuchi, Y. (1989). A simple culture method of fat cells from mature fat tissue fragments. *J. Lipid Res.* 30, 1987–1995.
- Sun, K., Kusminski, C.M., and Scherer, P.E. (2011). Adipose tissue remodeling and obesity. *J. Clin. Invest.* 121, 2094–2101.
- Tiraby, C., Tavernier, G., Lefort, C., Larrouy, D., Bouillaud, F., Ricquier, D., and Langin, D. (2003). Acquisition of brown fat cell features by human white adipocytes. *J. Biol. Chem.* 278, 33370–33376.
- Tontonoz, P., and Spiegelman, B.M. (2008). Fat and beyond: the diverse biology of PPARgamma. *Annu. Rev. Biochem.* 77, 289–312.
- Tran, T.T., and Kahn, C.R. (2010). Transplantation of adipose tissue and stem cells: role in metabolism and disease. *Nat. Rev. Endocrinol.* 6, 195–213.
- Trayhurn, P. (2013). Hypoxia and adipose tissue function and dysfunction in obesity. *Physiol. Rev.* 93, 1–21.
- Trayhurn, P. (2014). Hypoxia and adipocyte physiology: implications for adipose tissue dysfunction in obesity. *Annu. Rev. Nutr.* 34, 207–236.
- Uhlén, M., Fagerberg, L., Hallström, B.M., Lindskog, C., Oksvold, P., Mardinoglu, A., Sivertsson, Å., Kampf, C., Sjöstedt, E., Asplund, A., et al. (2015). Proteomics. Tissue-based map of the human proteome. *Science* 347, 1260419.
- Vitali, A., Murano, I., Zingaretti, M.C., Frontini, A., Ricquier, D., and Cinti, S. (2012). The adipose organ of obesity-prone C57BL/6J mice is composed of mixed white and brown adipocytes. *J. Lipid Res.* 53, 619–629.
- Waldén, T.B., Hansen, I.R., Timmons, J.A., Cannon, B., and Nedergaard, J. (2012). Recruited vs. nonrecruited molecular signatures of brown, “brite,” and white adipose tissues. *Am. J. Physiol. Endocrinol. Metab.* 302, E19–E31.
- Wang, Q.A., Scherer, P.E., and Gupta, R.K. (2014). Improved methodologies for the study of adipose biology: insights gained and opportunities ahead. *J. Lipid Res.* 55, 605–624.
- Wei, S., Bergen, W.G., Hausman, G.J., Zan, L., and Dodson, M.V. (2013). Cell culture purity issues and DFAT cells. *Biochem. Biophys. Res. Commun.* 433, 273–275.
- Wikswa, J.P. (2014). The relevance and potential roles of microphysiological systems in biology and medicine. *Exp. Biol. Med.* (Maywood) 239, 1061–1072.
- Wise, L.S., and Green, H. (1978). Studies of lipoprotein lipase during the adipose conversion of 3T3 cells. *Cell* 13, 233–242.
- Wu, X., Schneider, N., Platen, A., Mitra, I., Blazek, M., Zengerle, R., Schüle, R., and Meier, M. (2016). In situ characterization of the mTORC1 during adipogenesis of human adult stem cells on chip. *Proc. Natl. Acad. Sci. USA* 113, E4143–E4150.
- Yamamoto, Y., Gesta, S., Lee, K.Y., Tran, T.T., Saadatarad, P., and Kahn, C.R. (2010). Adipose depots possess unique developmental gene signatures. *Obesity (Silver Spring)* 18, 872–878.
- Yki-Järvinen, H. (2004). Thiazolidinediones. *N. Engl. J. Med.* 351, 1106–1118.
- Zuriaga, M.A., Fuster, J.J., Gokce, N., and Walsh, K. (2017). Humans and Mice Display Opposing Patterns of “Browning” Gene Expression in Visceral and Subcutaneous White Adipose Tissue Depots. *Front. Cardiovasc. Med.* 4, 27.

## STAR★METHODS

### KEY RESOURCES TABLE

| REAGENT or RESOURCE  | SOURCE                     | IDENTIFIER  |
|--|----------------------------|---|
| <b>Antibodies</b>  |                            |   |
| Anti-PPAR $\gamma$ (C26H12) Rabbit mAb                     | Cell Signaling Technology  | Cat#2435; RRID:AB_2166051   |
| Anti-HSL Rabbit pAb  | Cell Signaling Technology  | Cat#4107; RRID:AB_2296900   |
| Anti-HIF1 $\alpha$ Rabbit pAb                              | Novus Biologicals          | Cat#NB100-134; RRID:AB_350071   |
| Anti-Phospho AKT (Ser473) (D9E) XP <sup>®</sup> Rabbit mAb | Cell Signaling Technology  | Cat#4060; RRID:AB_2315049   |
| Anti-AKT (pan) (C67E7) Rabbit mAb                          | Cell Signaling Technology  | Cat#4691; RRID:AB_915783  |
| Anti-GFP Rabbit pAb  | Abcam                      | Cat#Ab290; RRID:AB_303395   |
| Anti-PGC1 $\alpha$ (H-300) Rabbit pAb                      | Santa Cruz Biotechnology   | Cat#SC-13067; RRID:AB_2166218   |
| Anti-UCP1 Mouse mAb  | R&D Systems                | Cat#MAB6158; RRID:AB_10572490   |
| Anti- $\beta$ -ACTIN (AC-15) Mouse mAb                     | Sigma Aldrich              | Cat#A5441; RRID:AB_476744   |
| Anti-TNF $\alpha$ (D2H4) Rabbit mAb                        | Cell Signaling Technology  | Cat#11969; RRID:AB_2797395  |
| <b>Bacterial and Virus Strains</b>                         |                            |   |
| Adeno-GFP  | Vector Biolabs             | Cat#1060  |
| Adeno-PGC1 $\alpha$  | Vector Biolabs             | Cat#ADV-219511  |
| <b>Chemicals, Peptides, and Recombinant Proteins</b>       |                            |   |
| Type 2 collagenase   | Worthington                | Cat#LS004177  |
| bFGF   | Sigma                      | Cat#F0291   |
| FGF21  | AstraZeneca                | N/A   |
| Irisin   | Enzo Life Sciences         | ADI-908-307-0010  |
| BMP7   | R&D                        | Cat#354-BP/CF   |
| BMP4   | R&D                        | Cat#314-BP-010/CF   |
| <b>Critical Commercial Assays</b>                          |                            |   |
| Human-proinflammatory panel 1                              | MesoScale                  | Cat#N05049A-1   |
| Mouse-proinflammatory panel 7                              | MesoScale                  | Cat#K15012B   |
| TrueSeq total library RNA prep kit                         | Illumina                   | Cat#RS-122-2303   |
| <b>Deposited Data</b>                                      |                            |   |
| Adipose and Adipocyte RNA Seq                              | This paper                 | GEO: GSE115020  |
| <b>Experimental Models: Cell Lines</b>                     |                            |   |
| RAW264 mouse macrophages                                   | AstraZeneca                | N/A   |
| <b>Experimental Models: Organisms/Strains</b>              |                            |   |
| Mouse: CD1   | Charles River              | Strain code:022   |
| <b>Oligonucleotides</b>                                    |                            |   |
| See <a href="#">Table S4</a> for primer sequences          |                            | N/A   |
| <b>Software and Algorithms</b>                             |                            |   |
| BCBIO  |                            | <a href="https://github.com/bcbio/bcbio-nextgen">https://github.com/bcbio/bcbio-nextgen</a>   |
| Hisat2   | Kim et al., 2015           | <a href="https://ccb.jhu.edu/software/hisat2/index.shtml">https://ccb.jhu.edu/software/hisat2/index.shtml</a>   |
| Sailfish   | Patro et al., 2014         | <a href="http://www.cs.cmu.edu/~ckingsf/software/sailfish/downloads.html">http://www.cs.cmu.edu/~ckingsf/software/sailfish/downloads.html</a>                         |
| DESeq  | Anders and Huber, 2010     | <a href="https://bioconductor.org/packages/release/bioc/html/DESeq.html">https://bioconductor.org/packages/release/bioc/html/DESeq.html</a>                           |
| RDavidWebService   | Fresno and Fernández, 2013 | <a href="https://www.bioconductor.org/packages/devel/bioc/html/RDAVIDWebService.html">https://www.bioconductor.org/packages/devel/bioc/html/RDAVIDWebService.html</a> |
| <b>Other</b>   |                            |   |
| 24-well 6.5mm Transwell                                    | Corning                    | Cat#3413  |
| Individual 6.5mm Transwell                                 | Corning                    | Cat#3397  |
| Individual 24mm Transwell                                  | Corning                    | Cat#3412  |

## CONTACT FOR REAGENT AND RESOURCE SHARING

Further information and requests for resources and reagents should be directed to and will be fulfilled by the Lead Contact, Jeremie Boucher ([Jeremie.Boucher@AstraZeneca.com](mailto:Jeremie.Boucher@AstraZeneca.com)).

## EXPERIMENTAL MODEL AND SUBJECT DETAILS

### Animals

6-week old female CD1 mice were obtained from Charles River, Germany. All animal experiments were approved by the Gothenburg Ethics Committee for Experimental Animals in Sweden.

### Human adipose

Anonymous samples of adipose tissue were collected from the abdominal region of female patients undergoing elective surgery at Sahlgrenska University Hospital in Gothenburg, Sweden. All study subjects received written and oral information before giving written informed consent for the use of the tissue. The studies were approved by The Regional Ethical Review Board in Gothenburg, Sweden. The donors had an average pre-operation BMI of 24.6. Human adipose tissue in [Figures 1D](#), [1E](#), [S1D](#), [3A](#), and [3B](#) were obtained from patients undergoing abdominal operations with uncomplicated gall-stone disease, inguinal hernia, or bariatric surgery from Ersta hospital in Stockholm. All subjects gave informed consent for anonymous use of the tissue. Lean patients were defined by a BMI < 26, while obese patients had a BMI > 30.

### Cell Lines

Murine macrophage RAW264 cells were cultured in DMEM/F12, 10% FBS, and 1% PennStrep.

## METHOD DETAILS

### Mouse adipose

Mature white adipocytes were isolated from CD1 female mice. Briefly, iWAT and eWAT depots were removed from the animals, minced finely, and digested in DMEM/F12 containing 1.5 U/ml of Collagenase D (Roche-11088866001) and 2.4 U/ml of Dispase II (Sigma-D4693) for approximately 30 minutes for the iWAT and 20 minutes for the eWAT. Digested material was passed through a 100  $\mu$ m filter (Falcon-352360), washed with DMEM/F12 +10%FBS and spun at 50 g x 3min. The medium was removed and the floating mature adipocytes were washed again.

### Human adipose

The adipose tissue was removed of fibrous material, finely minced, and digested in collagenase buffer containing HBSS +CaCl<sub>2</sub>+MgCl<sub>2</sub> (GIBCO 14065-49), 2% BSA, and 800U/g of tissue (~3mg/g of tissue) of type 2 collagenase (Worthington-LS004177) for approximately 40 min at 37°C. Digested material was passed through a 250  $\mu$ m strainer and washed 3 times with a total of 1L of KRHB buffer (1x KRH, 25mM HEPES, 2mM glucose, 2%BSA) using a separation funnel (VWR 527-0008 (or VWR 527-0005 for small scale preparations)) to separate the infranatant which contains the preadipocytes from the floating mature adipocytes.

### Membrane Setup

How to set up the MAAC cultures is schematized in [Figure S6](#). Both mouse and mature human adipocytes were spun at 50 g for 3 minutes to pack the cells, creating 3 layers: free lipid, mature adipocytes, and wash buffer. An 18-gauge needle and syringe were used to remove the free lipid and wash buffer. Of note, this step is crucial to getting a clean preparation and ultimately experimental reliability and reproducibility. If lipid or wash buffer remains the packed adipocytes will have a reduced surface tension, thus when inverting the membrane plates, adipocytes will drip-off, yielding inconsistent plating. All membrane experiments were performed using 0.4  $\mu$ m pore inserts. 6.5mm Transwells (Costar-3413 and 3397) were used for all mRNA and imaging experiments. 24mm transwells (Costar-3412) were used for protein experiments. Transwells were taken out of packaging and placed upside down (the canonical bottom facing the ceiling). Using a wide-bore tip, 30  $\mu$ L of packed human (approximately 60,000) or mouse adipocytes were pipetted onto each well. The transwells were picked up, inverted, and placed into a well containing 0.5-1ml of medium (DMEM/F12, 10%FBS, 1%Penn/Strep). If all free lipid and wash buffer has been removed, the cells will remain attached during the inversion. Cells were cultured for given lengths of time, with medium changed every 7 days. 1 mL of packed cells were used on 24 mm transwells (for protein and lipolysis) and cultured with 6 mL of medium.

### Preadipocyte Isolation and differentiation

Briefly, after digestion with collagenase, the infranatant containing the human stroma vascular cells were spun at 1000 RPM for 5 minutes, the buffer was removed and the pellet was resuspended in 5-10ml of red blood cell lysis buffer for 5 minutes. The pellet was spun at 1000 RPM for 5 minutes, resuspended in basal medium (ZenBio BM-1), 10% FBS, 1% Penn/Strep, 1nM bFGF (Sigma-F0291)

and seeded in flasks at a density of 20,000 per cm<sup>2</sup>. The cells were allowed to recover and expand for 5 days changing the medium every other day. The cells were trypsinized and seeded at 12,500 cells per well of a 96 well plate in proliferation medium EBM-2 (Lonza CC-3156) supplemented with EGM-2 MV SingleQuot Kit Supplements (Lonza CC-4147). After becoming confluent (usually 2-3 days), cells were differentiated in basal medium (Zenbio BM-1) with 3% FBS Gold (PAA-A15-104), 1% Penn/Strep, 1 μM pioglitazone, 0.5mM IBMX (Sigma-I5879), 1 μM dexamethasone (Sigma-D2915) and 100nM insulin (Novo Nordisk – Actrapid). After 7 days of differentiation, the medium was changed without the addition of pioglitazone or IBMX.

### Cell Culture

Explant cultures were obtained by finely mincing whole adipose into pieces of approximately 20mg, and cultured in DMEM/F12, 10% FBS, 1% Penn/Strep, 1 piece per 1ml/well for mRNA analysis, and 3 pieces per 6ml/well for protein. The medium was changed every 7 days, as was performed on the membrane cultures. Ceiling cultures (CC) were obtained by adding 1ml of packed cells to a T25 flask filled to the top (approximately 60ml) with DMEM/F12, 10%FBS, 1% Penn/Strep. The flask was inverted a number of times to ensure the adipocytes were well mixed and formed an even monolayer. If an air bubble was observed, the flask was momentarily shifted to capture the bubble in the cap. After 1 week the cells were adherent and the flask was inverted. Floating adipocyte experiments were performed by adding 30 μL of packed cells to 1ml of medium. Experiments involving hypoxic conditions were conducted in incubators set to 0.7% O<sub>2</sub>. GFP (Vector Biolabs-1060) and PGC1α (Vector Biolabs-ADV-219511) adenovirus were added to medium overnight, the medium was changed the following morning, and the cells were harvested after 7 days. FGF21 (AstraZeneca human WT-6His-FGF21 (1050ng/ml)), BMP7 (R&D 354-BP/CF (50ng/ml)), BMP4 (R&D 314-BP-010/CF (10ng/ml)), Irisin (Enzo Life Sciences ADI-908-307-0010 (1300ng/ml)), Rosi (1 μM), and T<sub>3</sub> (Sigma -T2877 (2nM)) were added to medium for 7 days in the presence of 20nM of insulin. The agonists rosiglitazone, dexamethasone, and GW3965 were all used at a final concentration of 10 μM (Figure 4). Rosiglitazone and GW3965 were obtained from AstraZeneca's compound management.

### Real-Time PCR and Western Blot Analysis

Total RNA was extracted from MAAC by aspirating the medium and adding 500 μL of TRIzol (Invitrogen-15596026). The TRIzol was pipetted up and down to dislodge all cells and incubated for 5 minutes, followed by purification using RNeasy Mini Kits (QIAGEN-74106). Isolated RNAs were reverse transcribed using the High-Capacity cDNA Synthesis kit (Applied Biosystems-4368814) and gene expression was measured using real-time PCR with Power SYBR Green master mix (Applied Biosystems) or TaqMan Universal Master Mix (Applied Biosystems) on a Quantstudio 7 Flex Real-Time PCR machine (Applied Biosystems). Tata-binding protein (TBP) was used as an internal normalization control. Primer sequences are included in Table S4. Protein extracts were prepared from MAAC by aspirating the medium and using PBS to wash the mature adipocytes off of the membrane into the bottom of the well. Using a wide bore pipette tip the adipocytes were collected, washed with PBS, spun at 100 g x3 min, the infranatant was removed, and the cells were lysed with 500μl RIPA + protease inhibitor (Roche-04693159001). Dimethylxalylglycine (DMOG) (Sigma-D3695 (100 μM)) was included in lysis buffer when hypoxia was assessed. For insulin sensitivity experiments, protease inhibitor and PhosStop (Roche-04906845001) were added to the lysis buffer. Explants were placed in a tissue lyser with a ball bearing and lysed for 1 minute. Adipocytes in RIPA were snap frozen and thawed rapidly at 90°C twice and spun at 10,000 g x 5 min at 4°C. The clarified lysate was removed from lipid and pellet, and spun again at 10,000 g x 5 min at 4°C to remove all remaining carryover lipid. Proteins were separated on 4%–12% Bis-Tris NuPAGE gels (Invitrogen) and transferred to PVDF membranes. Primary antibodies were PPARγ (Cell Signaling-2435), LIPE (Cell Signaling-4107), HIF1α (Novus-NB100-134), pAKT (Cell Signaling-4060), AKT (Cell Signaling-4691), GFP (Abcam-Ab290), PGC1α (Santa Cruz-SC-13067), UCP1 (R&D-MAB6158), and β-ACTIN (Sigma-A5441). Bands were detected using either standard ECL substrate (Pierce-32106) or SuperSignal West Femto (Thermo-34096).

### Functional Assays

Insulin sensitivity experiments were performed by removing adipocytes from the membrane and washing 2x with DMEM/F12 and placing the adipocytes in 2ml of DMEM/F12 in a 5ml tube. The cultured adipocytes were serum starved in the 5ml tube for 5 hours in a tissue culture incubator and were acutely stimulated with 100nM of insulin for 10 minutes. The cells were briefly spun, washed with ice-cold PBS and lysed in RIPA buffer containing protease inhibitor and PhosStop. Control cells were seeded on membranes and allowed to recover overnight in DMEM/F12/ 10%FBS and were run the day after isolation. All other aspects of the experiment were identical to the day 7 time point.

Glucose uptake experiments were performed by serum-starving the cultured adipocytes for 6 hours in Krebs-Ringer Bicarbonate Buffer (KRBB) (25mM HEPES (GIBCO)) supplemented with 2% fat-free BSA. 400μl of a 10% adipocyte KRBB mixture (40μl adipocytes/360μl KRBB) was preincubated with the indicated amount of insulin for 15 minutes while shaking at 37°C. Non-specific binding controls received 50μl of 200μM Cytochalasin B (Sigma-C2743). 40μl of a 1mM Deoxyglucose solution containing 8μCi/ml of <sup>14</sup>C Deoxyglucose (PerkinElmer-NEC720A250UC) was added to the cells for 10 minutes. Glucose uptake was halted by the addition of 50μl of Cytochalasin B. 250μl of cell suspension was added to thin separation tubes (Beckman Coulter-314326) containing 150μl of silicon oil (AS-100(Corning-10834)). Samples were spun at 10,000 g for 30 s. The tubes were cut in the middle in the oil phase, keeping the adipocytes on top of the oil, and discarding the bottom of the tubes which contained the the medium and radioactivity not incorporated into adipocytes. The adipocytes were solubilized in scintillation fluid (PerkinElmer-1200.437) and counted on a scintillation counter (BeckmanCoulter-LS 6500). 400μl of the 10% adipocyte KRBB mixture was additionally lysed in 1ml Dole solution

(78% 2-propanol, 20% heptane, 2% 1N H<sub>2</sub>SO<sub>4</sub>). The suspension was vortexed, incubated for 10 minutes, and 1 mL of heptane was added, followed by vortexing and another 10-minute incubation. 800 $\mu$ l of the organic phase was placed in a tared vial. Upon organic phase evaporation, the vial was weighed to determine total lipid per sample. Counts per minute (CPM) of each sample relative to CPM of the glucose solution was used to calculate nmol of glucose uptake. Uptake was normalized by lipid content. Cytochalasin control values were subtracted to determine glucose uptake. Control cells were treated as described above.

Lipogenesis experiments were conducted by serum-starving the cultured adipocytes for 6 hours in Krebs-Ringer Bicarbonate Buffer (KRBB) (25mM HEPES (GIBCO)) supplemented with 2% fat-free BSA. 500 $\mu$ l of a 10% adipocyte KRBB mixture (50 $\mu$ l adipocytes/450 $\mu$ l KRBB) was preincubated without insulin (basal) or 100nM insulin for 10 minutes while shaking at 37°C. 50 $\mu$ l of a 1.4mM glucose solution containing 1 $\mu$ Ci/ml of <sup>14</sup>C D glucose (PerkinElmer-NEC042V25OUC) was added to the cells for 90 minutes. The reaction was stopped by the addition of 1 mL of Dole solution. The suspension was vortexed, incubated for 10 minutes, and 1 mL of heptane was added, followed by vortexing and another 10 minute incubation. 800 $\mu$ l of the organic phase was placed in a scintillation vial, where after evaporation, it was solubilized in scintillation fluid and counted on a scintillation-counter. 500 $\mu$ l of the 10% adipocyte KRBB mixture was additionally lysed in 1ml Dole solution and had lipids extracted as described above. The organic phase was placed in a tared vial, where after evaporation, the vial was weighed to determine total lipid per sample. CPM of each sample relative to CPM of the glucose solution was used to calculate nmol of glucose incorporation. Lipogenesis was normalized by lipid content. Control cells were treated as described above.

Lipolysis experiments were performed on membrane cultured adipocytes that were washed in Krebs-Ringer Bicarbonate Buffer (KRBB) (25mM HEPES (GIBCO), 2mM Glucose) supplemented with 2% fat-free BSA prior to transfer of 5 $\mu$ l cell suspension per well into a 384-well polypropylene micro-titerplate (Greiner Bio-One 781280) using a Biomek FX autosampler workstation (Beckman Coulter). Lipolysis was stimulated by adding 40 $\mu$ l KRBB containing 0.002-100 $\mu$ M forskolin (Calbiochem, 10 concentrations in 1:3 dilutions) or 0.02-1000nM isoproterenol (Sigma-I6504, 10 concentrations in 1:3 dilutions) in 4 replicate wells. Adipocytes were incubated in a humidified 37°C shaker for 90 minutes after which glycerol content was measured by transferring 14 $\mu$ l of medium without adipocytes into new plates, and mixing it with 60 $\mu$ l of glycerol reagent (Sigma) according to the manufacturer's instruction. Plates were incubated for 7 minutes at 37°C and glycerol levels measured as absorbance at 540 nm. Basal lipolysis was calculated by assessing the level of lipolysis in the DMSO controls and divided by the levels found in cells treated with 30 $\mu$ M of the HSL inhibitor AZ compound 3. The amount of glycerol release for the compounds tested were calculated as % stimulation of glycerol release in relation to max (isoproterenol) and min stimulation (DMSO) using a logistic curve fit model (XLfit). Control cells were treated as described above.

### Co-Culture

Murine macrophage RAW264 cells were seeded on top of the membranes at a density of 100,000 per well, 6 hours later the medium was changed and the cells were treated with LPS (O26:B6) (Sigma- L8274) at a final concentration of 10ng/ml for 18 hours. The culture medium was collected and cytokine levels were measured using Mesoscale multiplexed ELISAs (Human-proinflammatory panel 1-N05049A-1), (Mouse-proinflammatory panel 7-plex-K15012B). Conditioned medium was generated by treating RAW264 cells (100,000/well) with LPS (10ng/ml) for 18 hours. Neutralizing TNF $\alpha$  antibody (Cell Signaling-11969) was used at final concentrations of low 100ng/ml, medium 250ng/ml, and high 1mg/ml and was incubated with the conditioned medium for 2 hours at room temperature before the medium was added to the adipocytes.

### Imaging

Adipocytes were fixed for 15 minutes in 4% formaldehyde, stained with bodipy (ThermoFisher-D3922 (25  $\mu$ g/ml)), hoechst 33342 (ThermoFisher-H3570 (2  $\mu$ g/ml)), and Cell Mask Deep Red (ThermoFisher-C10046 (1:1000)) for 30 min at room temperature and were subsequently washed 2x with PBS. Confocal imaging (Figure 2B) was performed using a Yokogawa CV7000s automated, spinning disc, confocal microscope (Wako automation, San Diego, California, USA) fitted with an Andor Zyla camera (Oxford Instruments, UK; unbinned pixel resolution of 0.1625  $\mu$ m/pixel). For the D0 floating and 2 week MAAC, optical slices were imaged using 2x2 binning and a 20x long working distance air objective (Olympus LUCPLFLN, NA 0.45) over a 240  $\mu$ m range at 20  $\mu$ m intervals, starting 600  $\mu$ m above the well bottom. The images are presented as maximum intensity projections. Similarly, preadipocyte and differentiated preadipocyte cultures were imaged using the same objective, and optical slices over a range of 60  $\mu$ m at 6  $\mu$ m intervals and these are also presented as maximum intensity projections. Imaging on ceiling cultures and MAAC as presented in Figure S1C were taken on a Nikon Eclipse TE2000-U inverted microscope. Viability was determined by washing cultured adipocytes 3x with PBS, then incubating with Calcein-AM (ThermoFisher- L3224 (10 $\mu$ M)) and propidium iodide ((Invitrogen-P3566 (2 $\mu$ g/ml)) at 37°C for 4 hours. After removing the staining solution, adipocytes were washed once with PBS and analyzed using an inverted Zeiss LSM 710 confocal microscope (Carl Zeiss AG, Oberkochen, Germany). For live/dead cell quantification, culture medium was aspirated, adipocytes were washed with PBS, and incubated in propidium iodide (2 $\mu$ g/ml) and Hoechst 33342 (2 $\mu$ g/ml) in PBS for 30 min at 37°C. The staining solution was aspirated and the membrane/cells were lifted out of the well and were gently placed in contact with a slide, transferring approximately 80% of cells. A 100 $\mu$ m spacer (Sigma-GBL654006), 50 $\mu$ l of PBS, and a coverslip were added. Quantifications were performed by counting the number of adipocytes containing PI positive nuclei versus Hoechst positive nuclei using an inverted Zeiss LSM 710 confocal microscope.

### RNA-Sequencing

RNA quality and quantity was assessed using a Fragment Analyzer standard sensitivity RNA kit (AATI # DNF-471) according to manufacturer's instructions. Libraries were prepared using Illumina's stranded total RNA library prep kit with "ribo-gold" rRNA depletion (catalog# RS-122-2303). The quality of the libraries were assessed using a Fragment Analyzer standard-sensitivity NGS kit (AATI # DNF-473). Samples were pooled so that they were present at an equal molarity. Pooled samples were sequenced 2x with NextSeq high output 150cycle kits (Illumina # FC-404-2002), paired-end reads. Quantification of the data was done using BCBIO version 1.0.1 (<https://github.com/bcbio/bcbio-nextgen>). Hisat2 version 2.0.5 (Kim et al., 2015) was used within BCBIO to align the data against the human hg38 assembly, thereby the number of aligned reads ranging between 1.5M and 38M. Sailfish 0.10.1 (Patro et al., 2014) was used within BCBIO to quantify gene counts.

### Bioinformatics

RNA-Seq data was compared via PCA analysis after log-transformation ( $\log_{10}$  count + 0.01). Pearson's correlation coefficients of log-transformed averaged gene expression per condition were calculated to determine clustering of different conditions and the direct comparison of starting material with the different culture methods. To identify differentially expressed genes of each model relative to the starting material, we performed negative binomial tests by DESeq software (Anders and Huber, 2010) and chose the most significant genes per conditions ( $FDR < 1 \times 10^{-8}$ ). We also found enriched GO terms of DEGs per conditions by DAVID at the statistical significance of  $FDR < 1 \times 10^{-3}$  (Fresno and Fernández, 2013; Huang et al., 2009). We plotted enriched GO terms as a network after clustering based on Jaccard similarity of overlapped genes, enabling simpler interpretation, such as an Enrichment Map (Merico et al., 2010). We calculated how much those terms were enriched in upregulated or downregulated genes (polarity - Table S2); counting conditions enriched in upregulated genes and subtracting conditions enriched in downregulated genes. We also checked in which conditions those terms were specifically enriched in, (generality - Table S2); counting all conditions enriched in upregulated genes or downregulated genes.

### QUANTIFICATION AND STATISTICAL ANALYSIS

All data are reported as mean  $\pm$  standard deviation. The reported n in figure legends refers to the number of biological replicates of samples tested in each experiment. Statistics in Figure 3, S3, and 6C were calculated using an unpaired 2-tailed t test (Prism). All other statistics were calculated using a one-way ANOVA with Dunnett's Multiple Comparison test (Prism). (mean  $\pm$  stdev, \*p < 0.05; \*\*p < 0.01; \*\*\*p < 0.001)

### DATA AND SOFTWARE AVAILABILITY

The accession number for the RNA-Sequencing data reported in this paper is GEO: GSE115020.